Received: 8 September 2020 | Revised: 9 April 2021 | Accepted: 2 June 2021

DOI: 10.1002/suco.202000571

TECHNICAL PAPER

fib CEB-FIP WILEY

Investigation of impact behavior of reinforced concrete beam to column connection strengthened with carbon fiber-reinforced polymer strips

Turgut Kaya[1] | Murat Aras[2] | Tolga Yilmaz[3] | Özlem Çalişkan[2] | Özgür Anil[4] | R. Tuğrul Erdem[5]

[1]Department of Civil Engineering, Batman University, Batman, Turkey

[2]Department of Civil Engineering, Bilecik Şeyh Edebali University, Bilecik, Turkey

[3]Department of Civil Engineering, Eskisehir Osmangazi University, Eskisehir, Turkey

[4]Department of Civil Engineering, Gazi University, Ankara, Turkey

[5]Department of Civil Engineering, Manisa Celal Bayar University, Manisa, Turkey

Correspondence
Özgür Anil, Department of Civil Engineering, Bilecik Şeyh Edebali University, Bilecik, Turkey.
Email: oanil@gazi.edu.tr

Abstract

Reinforced concrete (RC) members may expose to impulsive dynamic loads due to the reasons such as the explosions occurring in the interior or exterior part of them, rockfall, the vehicle crash to the bridges, the collision of masses with the effects of floods and landslide. Many studies have investigated the effects of impulsive dynamic loads on the beam, column, and slab RC structural elements have been investigated in the literature. However, the authors have not encountered any study focused on the impact behavior of beam to column connections of the frames constructing the bearing system of reinforced concrete structures. Therefore, an experimental study has been planned to investigate RC beam impact behavior to column connections strengthened with carbon fiber-reinforced polymer (CFRP) strips. The concrete compressive strength, shear reinforcement spacing, CFRP strip spacing, and input impact energy applied to test specimens were taken as experimental variables. The time histories of impact load acting on test specimens, accelerations, displacements, and the strains measured from CFRP strips have been recorded in experiments. The experimental variables' effect on dynamic responses of RC beam to column connections strengthened with CFRP strips subjected to impact load has been interpreted in detail. The study's scope and improved numerical analysis procedure have also been introduced to verify experimental results. Good agreement between numerical and experimental results demonstrated that the presented numerical procedures could be safely used for evaluation of impact behavior of RC beam to column connections strengthened with CFRP strips.

KEYWORDS

beam to column connection, CFRP, free drop test, impact load, strengthening

1 | INTRODUCTION

The conventional design of RC structures has been performed by considering the dynamic loads such as

Discussion on this paper must be submitted within two months of the print publication. The discussion will then be published in print, along with the authors' closure, if any, approximately nine months after the print publication.

earthquake and wind and the vertical static loads. However, RC structures may subject to impulsive impact loads due to different reasons in their service period. One of the most common cases is spherical air-shock wave generated by explosions on structures as the dynamic impulsive load. Impulsive impact load effects can be seen in the inner part of structures due to explosions that accidentally occurred in the natural gas tanks or LPG gas tanks. Besides, military structures or buildings that have strategic importance may expose to impulsive impact load in their outer environment with explosions due to terrorist attacks. Furthermore, rockfall, the collision of masses with the effect of flood and landslide, vehicle crashes to highway or seaway bridges are other reasons causing impact loads on structures. RC structures or structural members designed without considering the impact load effects may experience significant damage or total collapse. In order to prevent such situations, the behavior and performance of RC structures dynamic impact loads should be investigated and interpreted in detail.[1–3]

Many comprehensive experimental and analytical studies, where the impact behavior of the concrete or reinforced concrete beam, column, and slab structural elements is investigated, exist in the literature.[4–23] The impact behavior of beams manufactured using fiber reinforced concrete and beams strengthened with fiber-reinforced polymer strips have also been investigated.[24–33] Furthermore, under the effect of impulsive loads, the dynamic response and failure modes of ultra-high-performance fiber-reinforced concrete columns (UHPFRC), precast segmental columns, RC columns strengthened with fiber-reinforced polymer (FRP) composites, and concrete-filled steel tube (CFST) columns were investigated.[2,34–44] In the studies focused on RC slabs subjected to impact load, the effects of the reinforcement ratio, pre-stress, support conditions, and strengthening with FRP strips on dynamic responses of RC slabs have been examined.[45–49]

The detailed literature review conducted has unveiled many works in which impact behaviors of beams, columns, and slabs, which are structural members constructing RC frame structures, were investigated. However, the authors have not encountered any study focused on the beam's dynamic behavior to column connections of RC frame structures under the impulsive impact load. At the end of the literature review performed for the beam to column connections subjected to impact load, authors have come across only one study. This study, presented by Al-Rifaie et al.,[50] was related to the steel beam to column connections. In this study, analytically and experimentally investigated steel beam to column connections under quasi-static load and impact load is examined. The eight specimens designed as the partial depth end-plate connections and the flush plate connections were tested in the study. One of the study findings is that steel beam to column connections have experienced more energy absorption capacity during impact loading than quasi-static loading. Three stages characterized lateral impact response: (a) peak stage, (b) plateau stage, and (c) bounce stage, and it was found out that 60% of the plastic deformations occurred during the plateau stage. After comparing the static and impulsive loading, the dynamic increase factor (DIF) values have been proposed for predicting the effect of the dynamic impact loading. It is emphasized that the DIF values have changed between 1.25 and 1.38 for experiments and between 1.19 and 1.34 for the finite element analysis.

As mentioned above, as the result of the authors' detailed literature review, it has been seen that there is no study where the impact behavior of RC beam to column connections or RC beam to column connections strengthened with carbon fiber-reinforced polymer (CFRP) strips has been investigated. Therefore, an experimental study has been planned. In the study's scope, the concrete compressive strength used for the manufacture of the beam to column connections, the shear reinforcement spacing, the spacing of CFRP strips used for strengthening, and the input impact energy level applied to test specimens were taken as experimental variables. This study was aimed to examine the behavior of column-beam joints with insufficient shear reinforcement and very low concrete strength under the effect of sudden dynamic impact loading, which is needed to be strengthened. To what extent the strengthening techniques proposed with CFRP strips in reinforced concrete column-beam joints with low concrete strength and insufficiently shear reinforcement increase the performance level under the effect of sudden dynamic impact loading is the main issue in the study. It is known that reinforced concrete structures in need of reinforcement have very low concrete compressive strength values. For this reason, a concrete column-beam joint with a concrete strength of 10 MPa was selected in the experimental study. This study's main purpose is to examine the performance levels of reinforced concrete column-beam joints under the effect of sudden dynamic impact loading, which has different design errors and deficiencies and needs strengthening. The strengthening detail proposed in the study aimed to determine the extent to which the performance of insufficient column-beam joints under the effect of sudden dynamic impact loading can be increased. For this reason, the rebars used as shear reinforcement have been used as plain rebars as in the old structures that need strengthening. The 1/3 scaled 16 RC beam to column connection test specimens were

manufactured and tested under the impact load. The impact load was applied to test specimens using a drop-weight test setup designed by the authors. The time histories of impact load acting on test specimens, accelerations, displacements, and the strains measured from the CFRP strips have been measured during the tests. These measurements taken from specimens have been compared by interpreting. Furthermore, an improved numerical analysis procedure based on finite element analysis (FEA) was introduced. The dynamic responses and failure modes of test specimens were compared to those obtained via the presented FEA. The comments related to which extent the presented finite element model has been successful for evaluation of dynamic

TABLE 1 Properties of test specimens

Spec. no	Weight of hammer (kg)	Concrete compressive strength (MPa)	Drop height (mm)	Stirrup spacing (mm)	CFRP strip spacing (mm)
1	84	10	500	300	150
2					250
3				Without stirrup	150
4					250
5			750	300	150
6					250
7				Without stirrup	150
8					250
9		25	500	300	150
10					250
11				Without stirrup	150
12					250
13			750	300	150
14					250
15				Without stirrup	150
16					250

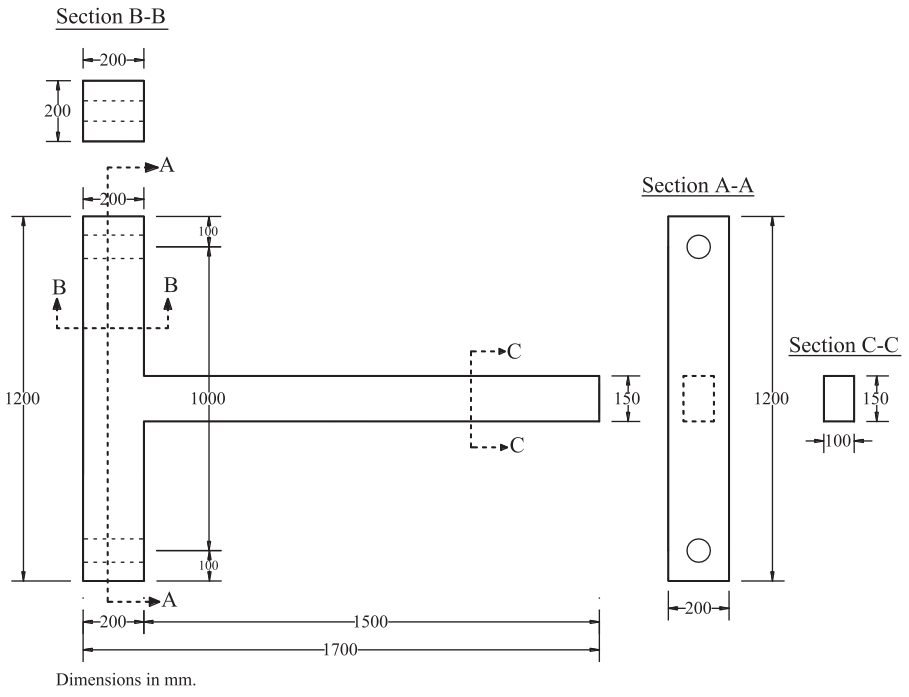

FIGURE 1 Dimensions of test specimens

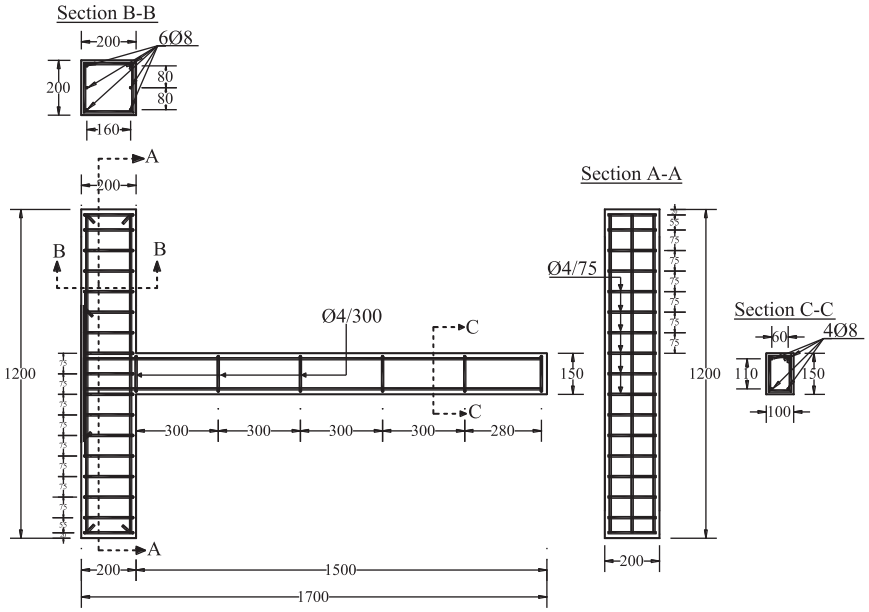

(a) Reinforcement detail of Specimens 1, 2, 5, 6, 9, 10, 13 and 14

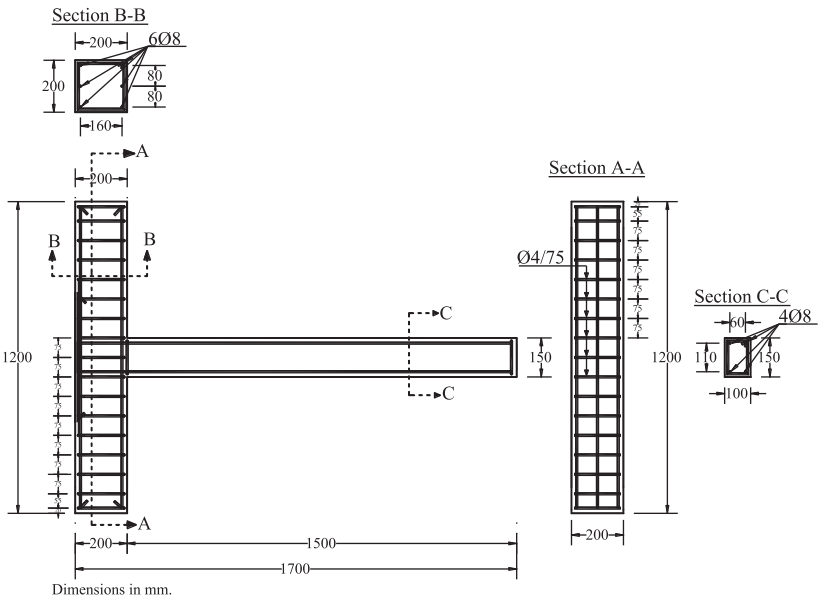

(b) Reinforcement detail of Specimens 3, 4, 7, 8, 11, 12, 15 and 16

FIGURE 2 Reinforcement detail of test specimens

impact behavior of RC beam to column connection elements were conducted.

2 | EXPERIMENTAL STUDY

2.1 | Test specimens and materials

The RC beam's impulsive impact behavior to column connections was investigated in the experimental study's scope. The investigated experimental variables were the concrete compressive strength, the shear reinforcement spacing, the CFRP strip's spacing, and the input impact energy level transmitted to test specimens. The properties of test specimens and the experimental variables were given in Table 1. Two series of test specimens whose compressive strengths were 10 and 25 MPa had been manufactured. The half of the beams constructing beam to column connections included shear reinforcements with the spacing of 300 mm. Remain beams constructing beam to column connections had been manufactured without the shear reinforcements. The beams of the RC beam to column connections have been designed as shear-deficient and manufactured. These beams that had

TABLE 2 Properties of CFRP Sikawrap 160-C (unidirectional) and resin Sikadur 330

Properties of CFRP	Remarks of CFRP[a]
Thickness (mm)	0.12
Tensile strength (MPa)	4100
Elastic modulus (MPa)	231,000
Ultimate tensile strain (%)	1.7
Properties of resin	Remarks of resin[a]
Tensile strength (MPa)	30
Elastic modulus (MPa)	3800

[a]These values are given by the manufacturer.

an insufficient quantity of shear reinforcement were strengthened with CFRP by wrapping externally. The spacing of CFRP strips bonded as the shape of "U" was 150 and 250 mm. Another experimental variable was the input impact energy level applied to the test specimen. Two different input impact energies were applied to test specimens by dropping the steel hammer with a weight of 84 kg from two different drop-heights, 500 and 750 mm.

The 1/3 scaled the RC beam to column connections used for the experimental program have represented the outer beam to column connection of standard RC frame structures. Designed test specimens correspond to the rotation points passing through the midpoints of the beam and column, which takes place in the RC frame structure's outer beam to column connection. The geometric dimensions of test specimens were presented in Figure 1. The targeted concrete compressive strengths were for 10 and 25 MPa for two different series. Five standard cube test samples with a dimension of 150×150 mm were taken from each test specimen and kept in similar curing conditions with RC beam to column connection test specimens to determine concrete compressive strength. The concrete cube samples were kept in the curing environment for 21 days with the test specimens and then allowed to dry in the laboratory for 7 days. The concrete compressive strength of cube samples was determined with axial compression tests on days when the experiments were conducted. The RC beam's average concrete compressive strengths to column connection test specimens had been determined as 10.3 and 24.8 MPa, which were quite close to the value of targeted concrete compressive strength. The concrete compressive strengths of test elements were obtained close to each other, and standard deviation and variation values were low. The tests of the test elements' concrete compressive strengths were made according to the Eurocode 2 regulation.[51] The reinforcements used in RC beam to column connections were provided simultaneously, and test specimens were manufactured with the same reinforcements. Reinforcement details were given in Figure 2. The column reinforcements were identical for whole test specimens.

The columns have included six longitudinal ribbed rebars with a diameter of 8 mm and the 4 mm diameter stirrup placed with a spacing of 75 mm. The stirrups were formed from plain rebars. The only difference in reinforcement details of the test specimens was the spacing of shear reinforcements in beams. Beams have included four longitudinal ribbed rebars with a diameter of 8 mm for all test specimens. The shear reinforcements were placed with the spacing of 300 mm in beams of Specimens 1, 2, 5, 6, 9, 10, 13, and 14. Remain specimens had no shear reinforcements. Five samples taken from reinforcements were tested under the axial tensile load to determine each type of reinforcements' mechanical properties. The elastic modulus, yield strength, and ultimate strength of the ribbed rebars with a diameter of 8 mm were $E = 209$ GPa, $f_{sy} = 485$ MPa, and $f_{su} = 569$ MPa, respectively. For shear reinforcements with a diameter of 4 mm, these mechanical properties were $E = 210$ GPa, $f_{sy} = 415$ MPa, and $f_{su} = 525$ MPa, respectively. The axial tensile tests of the reinforcement used in the test elements were carried out according to the ASTM A615-16 Standard Specification for Deformed and Plain Carbon-Steel Bars for Concrete Reinforcement.[52]

After the RC beam's manufacture to column connection test specimens completed, the CFRP material was preferred for strengthening the shear-deficient beam part. The CFRP strips and epoxy were the products of the Sika company. The mechanical properties of CFRP and epoxy, provided by the manufacturer, were given in Table 2. After completing the test specimens' curing time, the strengthening of test specimens' beam regions with CFRP strips was performed. The spacing of CFRP strips in the beams was preferred as 150 mm and 250 mm. The strengthening details were presented in Figure 3. Two side surfaces and bottom surfaces of beams belonging to RC beam-column joins, in which CFRP strips were bonded, have been roughened until the aggregates expose. Then these surfaces were cleaned with water-soaked sponges and were dried with compressed air. Two-part epoxy mixed up a point at which mixture took a single uniform color, and then a 0.5 mm thick epoxy was applied to the surfaces. A special hand tool with 0.5 mm teeth was used for applying epoxy on to the concrete surface. After that, CFRP strips were laid on to epoxy by hand carefully without changing the fibers' directions. Only one single layer of CFRP was used for the strengthening of specimens. These CFRP strips were soaked with epoxy to prevent air bubbles between the beam side and CFRP. Finally, another 0.5 mm thick epoxy was applied to CFRP strips to protect

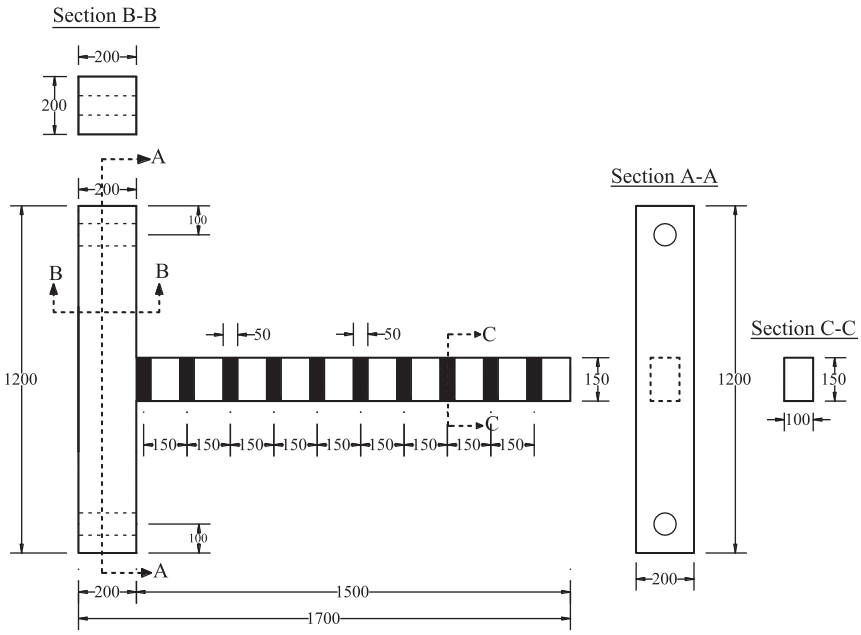

(a) Strengthening detail of Specimens 1, 3, 5, 7, 9, 11, 13 and 15

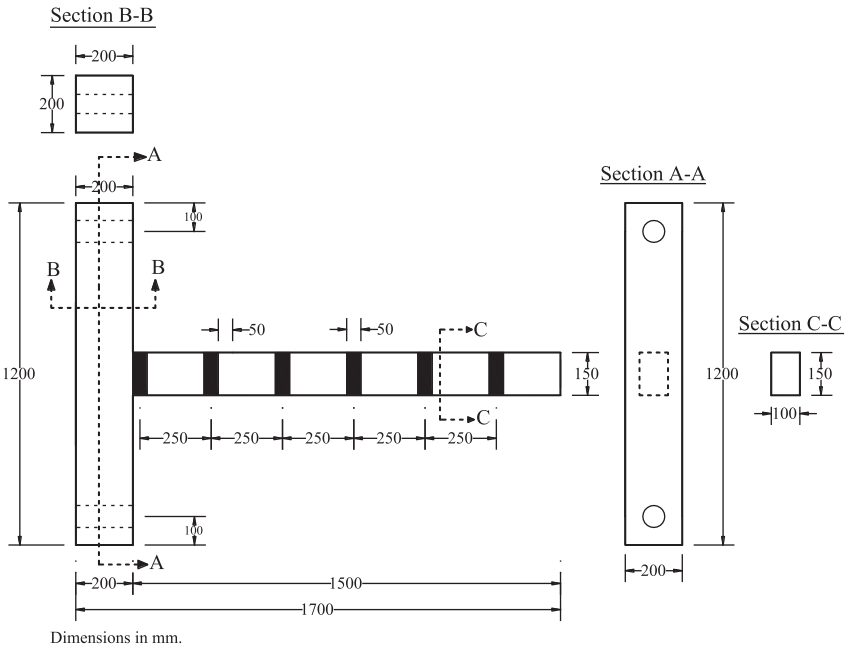

(b) Strengthening detail of Specimens 2, 4, 6, 8, 10, 12, 14 and 16

FIGURE 3 Strengthening details of test specimens

the fibers' direction. The explained strengthening technique was applied to all of the specimens identically. When the procedure mentioned above is applied, attention should be paid to keeping the laboratories' temperature around 20°C ± 2°C. After CFRP strips were bonded, a 7-day curing time was waited to reach the epoxy's full strength. The CFRP bonding to the concrete surface is strongly dependent on the proper application of the procedure and the surface preparation. Keeping the direction of fibers of CFRP strips and soaking the epoxy into CFRP while avoiding air bubbles are the key factors for bonding. The strengthening procedure should be done with great care for determining the impact behavior of specimens strengthened with CFRP strips completely.

2.2 | Test setup and instrumentations

Impact loading was applied to the RC beam to column connections using the drop-weight test setup presented in

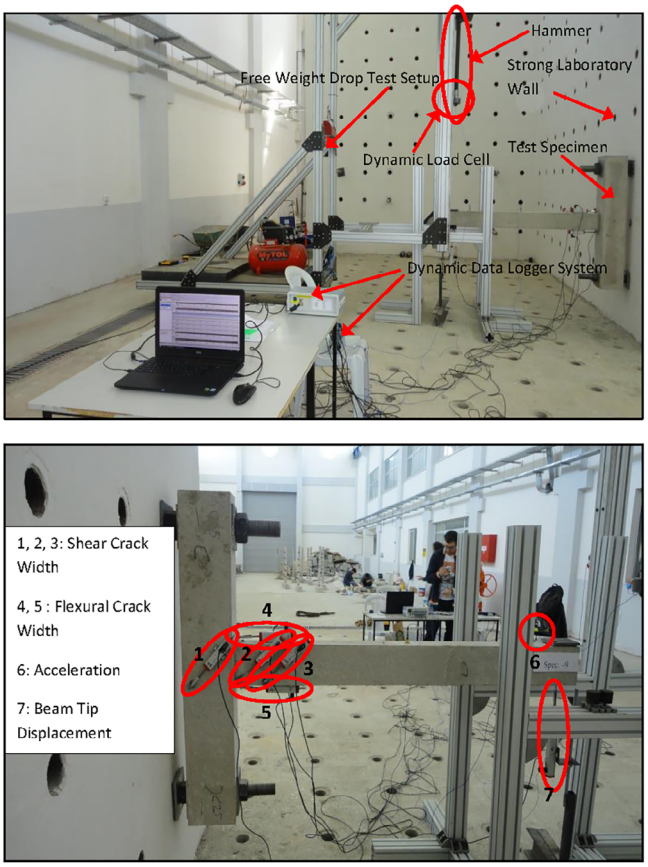

FIGURE 4 Test setup and instrumentations

Figure 4. This setup has been specifically developed for the impact experiments. The test setup allows the dropping different weights from a maximum height of 2500 mm to the test specimens with various dimensions. The weight of the hammer was kept constant during the tests. An 84 kg hammer was dropped from a height of 500 and 750 mm to apply impact loading to the same contact point. By this means, two different input energy level were applied to RC beam to column connection test specimens ($9.81 \times 84 \times 0.5 = 0.4120$ kJ and $9.81 \times 84 \times 0.75 = 0.6190$ kJ). In order to prevent local fractures at the point of contact and to obtain a load distribution, high strength steel plates with dimensions $100 \times 100 \times 10$ mm were placed on the contact points. The steel loading plates were fixed to the specimens with two mechanical anchors. Special polyurethane rubbers were also placed between the loading plates and test specimens.

RC beam to column joint specimens was placed into the impact test setup by supporting the rigid RC laboratory wall using high strength rods. As similar to their actual position, test specimens' columns were fixed to the rigid wall in vertical, and beams were placed to drop-weight test setup horizontally. The impact energy that will transmit to specimens, which have been adjusted by changing the hammer's weight and drop height, has been selected at the proper level to trace the damage that will occur in the specimens. The semi-spherical impact hammerhead used in experiments was fabricated from high-strength steel. The impact hammerhead's geometry was taken as constant in tests like dropping the weight of the hammer. In the experimental part of this study, impact loading applied to test specimens was measured by an ICP piezoelectric dynamic load cell placed into the hemispherical part of the drop weight hammer apparatus in the test setup. The accelerometer was also connected to the RC beam to column joint specimens to measure the vibration motions under the effect of impact loading. The accelerometers' objective was not to measure impact loading but to measure the vibration exhibited by specimens under impact loading. Under the effect of impact loadings with two different level input energies, test specimens' dynamic response was evaluated using this accelerometer's vibration characteristics. The piezoelectric accelerometer placed on the test specimens has a 5000 g capacity. This accelerometer has been placed on the RC beam's free edge close to the impact loading point. The accelerometer was fixed with special brass connection apparatus by using mechanical anchors.

Additionally, the displacement time histories of the six different points on the RC beam to column specimens have been measured. The whole of six displacement measurements was recorded for different purposes. One of the measurements was used to determine vertical displacements of the beam ends. For each specimen, three displacement transducers were placed on the beam and the column to beam joint zone with the angle of 45° to measure the width of the shear crack that will be able to occur. The other two displacement transducers were placed on top and bottom surfaces of the beam, as possible as close to the beam-column connection region, to measure the bending crack that will occur. The displacement measurements aim to measure all impact load-induced displacements such as beam end displacements, the shear cracks widths, and bending cracks widths.

Furthermore, time histories of strains measured from CFRP strips bonded to the side face of the RC beam part of the beam to column joint specimens for strengthening, and time histories of impact load acting on test specimens were measured. For each specimen, three strain measurements were taken from CFRP strips wrapped to beam in the shape of U. These measurements were taken from the first three CFRP strips, which were closest to the beam-column joint zone region. The data were obtained through a dynamic data logger system. Special software was used for this data logger system to perform the tests. One impact load, one acceleration, six displacement, and three strain measurements have been taken

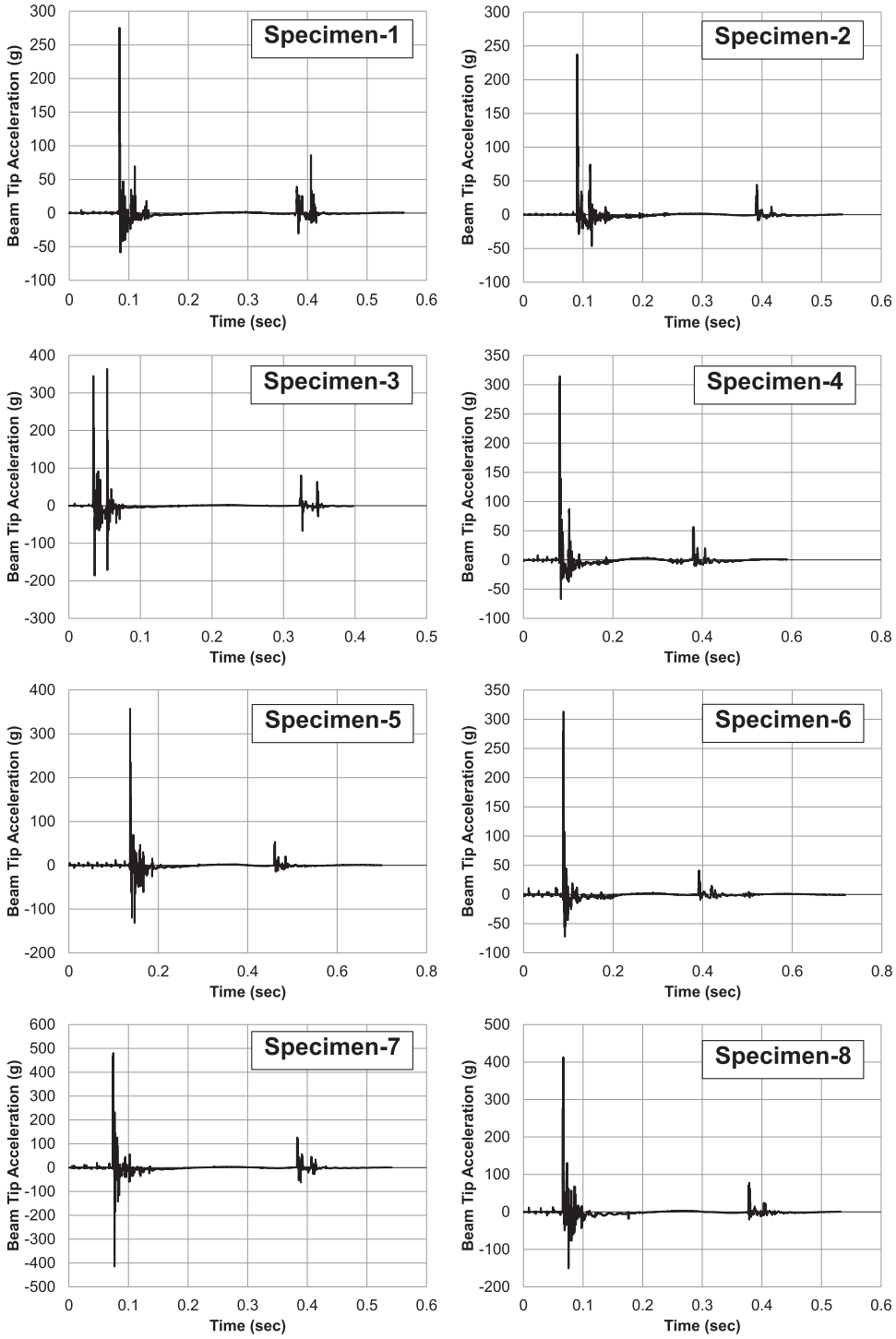

FIGURE 5 Beam tip acceleration–time graphs of specimens

from each test specimen using the dynamic data-logger system.

3 | EXPERIMENTAL RESULTS AND DISCUSSIONS

In the experimental study's scope, time histories of one acceleration, six displacements, three strain, and impact force applied to beam end were recorded to investigate and interpret the effect of the experimental variables on the impact behavior beam-column joints strengthened with CFRP strips. The time histories of the beam-end accelerations measured from test specimens and the impact loads applied to beam ends were given in Figures 5 and 6, respectively. Besides, the time histories of the beam-end displacements measured from the impact loading point were presented in Figure 7. It aims to interpret the strengthening method's effects by measuring the displacement and acceleration taken from the beam end

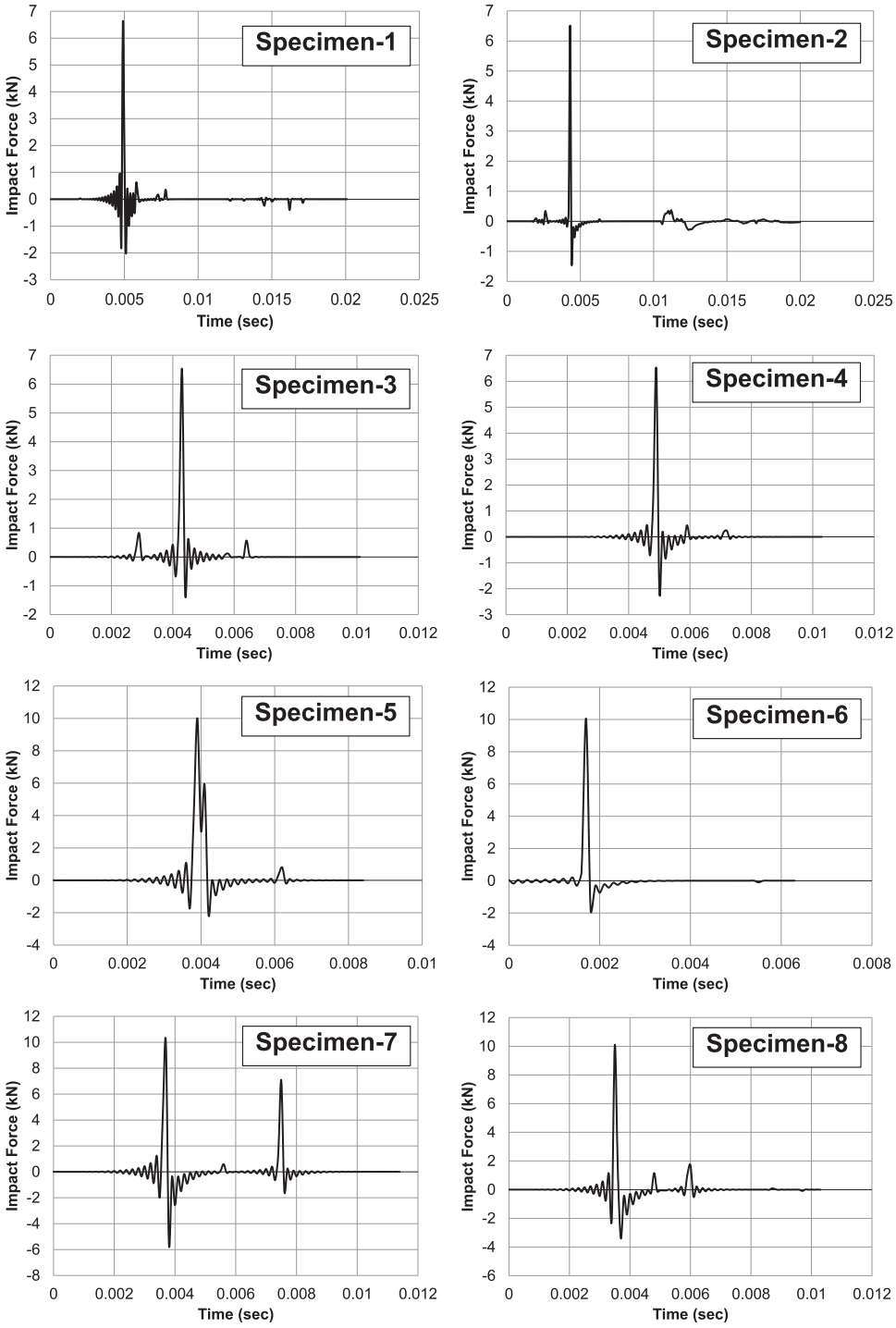

FIGURE 6 Impact load–time graphs of specimens

on reinforced concrete column beam joints' performance. The three shear crack widths-time measurements were taken from the intersection point of the beam to column zone, and the beam region of each beam to column connection specimen, and these graphs were presented in Figures 8–10. Shear crack widths given in Figure 8 were measured from the intersection point of the beam to the column zone and named as the number one shear measurement. The other two shear crack width measurements taken from beam regions were presented in Figures 9 and 10, and they were named measurements number two and three, respectively. The shear crack width with the number two was taken from the maximum moment region, while the number three was taken from a point closer to the beam end and near the point of number two. The shear crack measurements taken from the RC column-beam joint area aimed to determine the extent to which the shear crack widths caused by the impact load applied to the specimens affected the proposed strengthening method. Shear crack widths are an

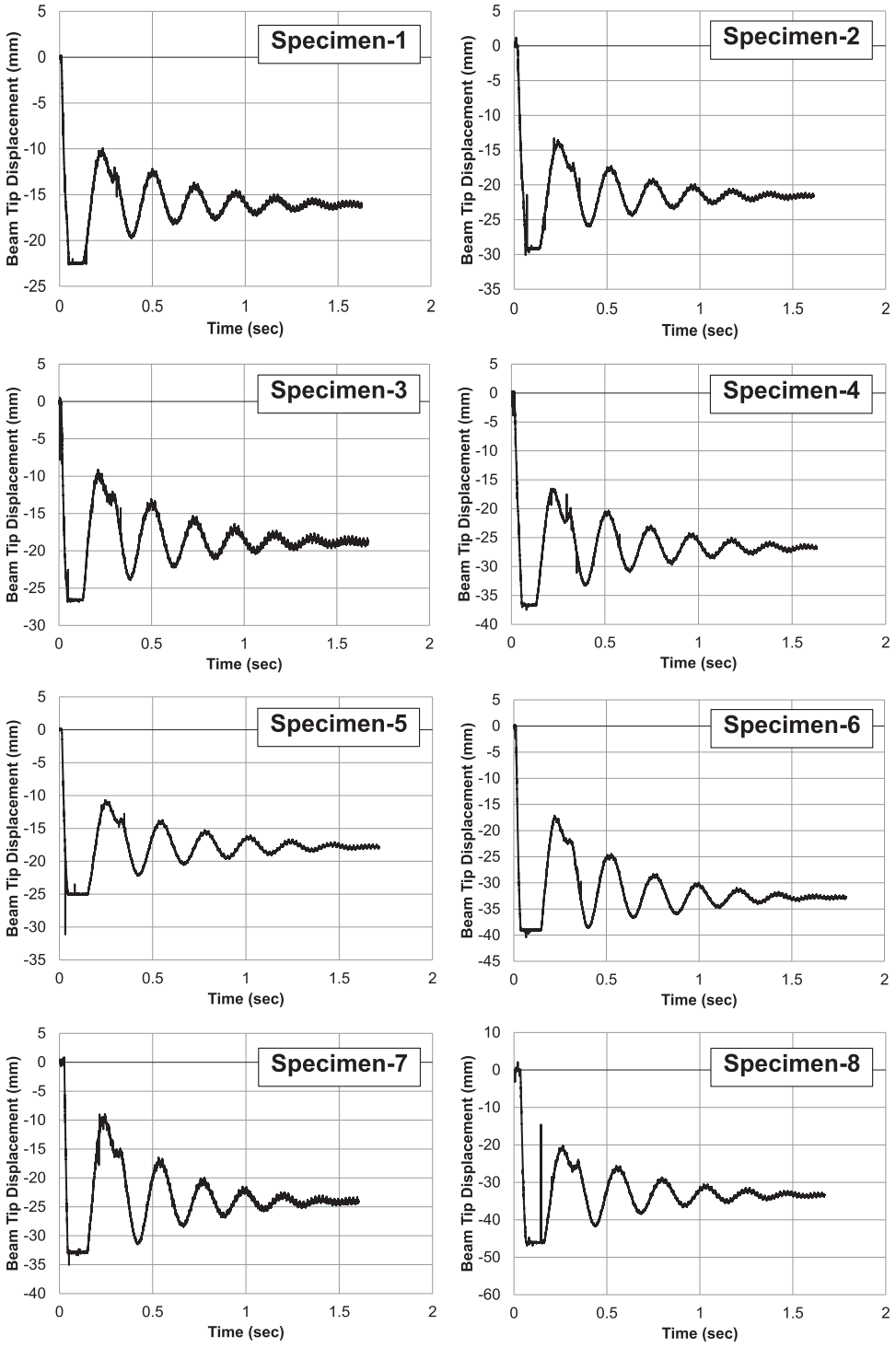

FIGURE 7 Beam tip displacement–time graphs of specimens

important indicator for determining the strengthening technique's performance level applied in column-beam joints where shear reinforcement is extremely insufficient, and shear reinforcement is not densified. Using the beam end displacement versus time distribution graph presented in Figure 7, it is interpreted how the strengthening method applied to the test elements with CFRP strips affects the behavior under impact loading. Likewise, by analyzing the shear crack width–time distribution graphs given in Figures 8–10, comments were made about how successful the strengthening method applied with CFRP strips in limiting the shear cracks in the reinforced concrete beam–column junction was made. Figures 11 and 12 show the variation of flexural crack widths measured from the bottom and top surfaces that were at maximum moment point according to time. Figure 11 shows the bottom surface flexural crack width, and Figure 12 shows the top surface flexural crack. For each test specimen, three strain

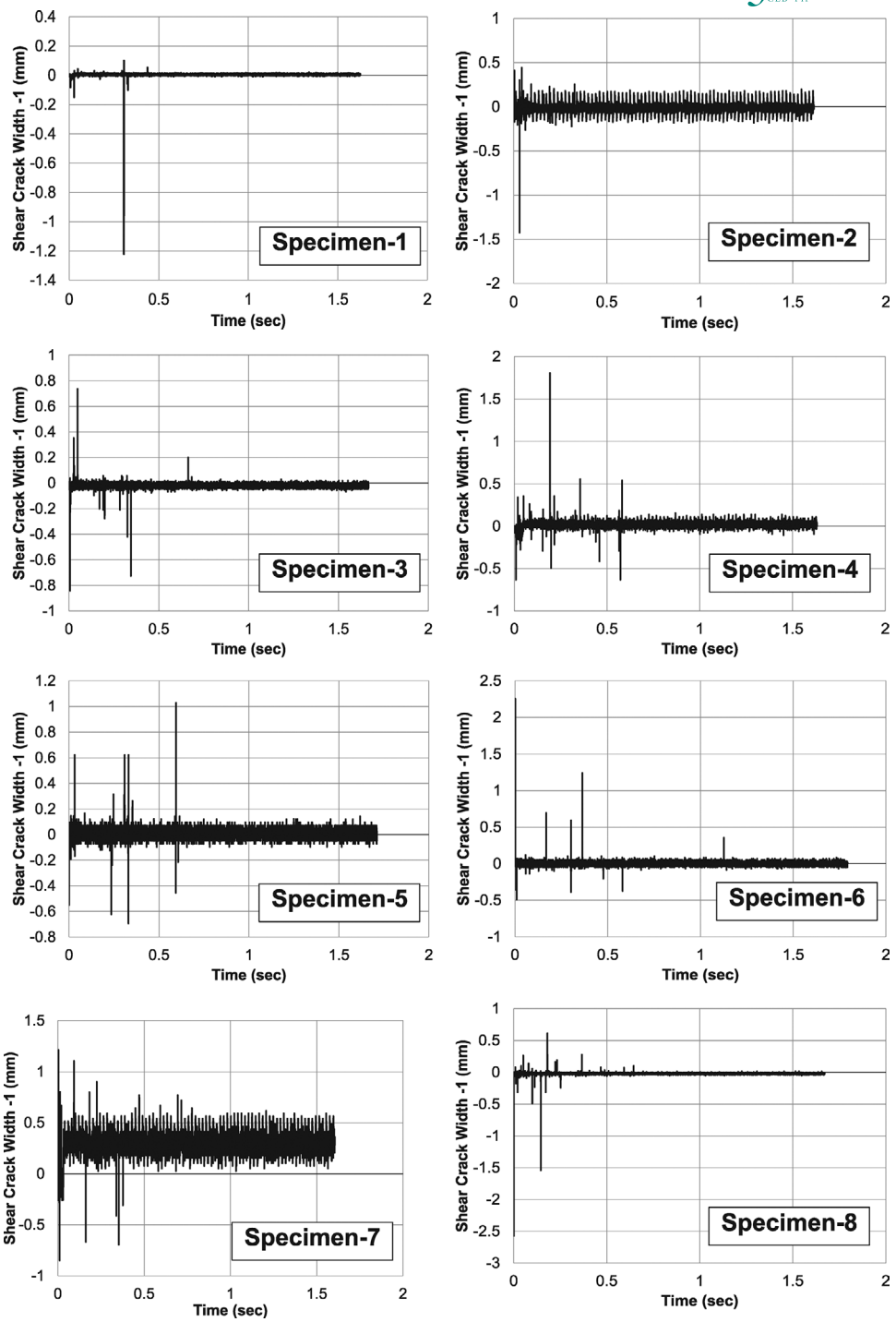

FIGURE 8 Shear crack width 1-time graphs of specimens

measurements were taken from three CFRP strips nearest the panel zone. The strain gauges were mounted on CFRP strips wrapped to side surfaces of the beam. Strain gauges were mounted on the mid-point of CFRP strips, which corresponds to the half of beam height, in the main bearing fibers' direction. The strain–time measurements, including maximum values of among three strain measurements, were presented in Figure 13. The results obtained by experiments are summarized in Table 3.

One of the variables investigated in the experimental study's scope is the spacing of CFRP strips used for strengthening the beam to column connection test specimens. CFRP strips were bonded to test specimens with the spacing of 150 and 250 mm. The increase of the CFRP strip's spacing decreased the maximum acceleration values measured from the end of the beam, on average, 16%. The increase of the CFRP strip spacing from 150 to 250 mm increased the maximum displacement values measured from beam end, the maximum shear crack width values, the maximum flexural crack width values, the residual displacement values at the beam end, and the maximum strain values measured

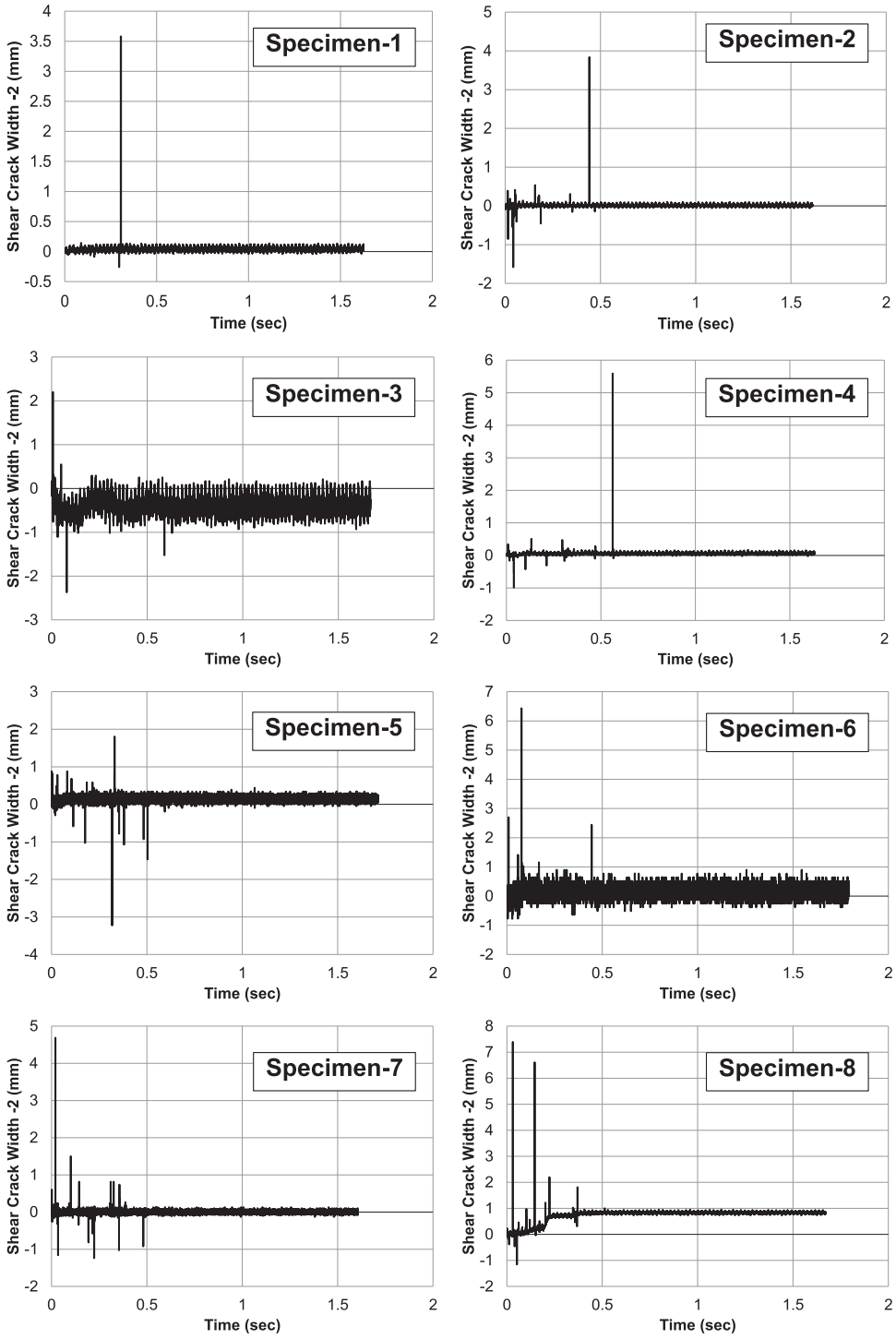

FIGURE 9 Shear crack width 2-time graphs of specimens

from CFRP strips as 36%, 43%, 39%, 55%, and 67%, respectively. The strengthening with CFRP strips remarkably improved the beam's performance to column connection areas under the impulsive impact loading effect. The CFRP strips enhanced the beam's stiffness and toughness to column connection test specimens, increased the maximum acceleration values that occurred due to impact loading, and considerably decreased the displacement and crack width values. CFRP strips highly decreased beam end displacement values and played an effective role in limiting the shear and flexural crack widths. Test Specimen strengthening using CFRP with the spacing of 150 mm experienced much better impact performance than those strengthening using CFRP with 250 mm. Strain values measured from test specimens with the CFRP spacing of 250 mm were obtained greater than those with the CFRP spacing of 150 mm.

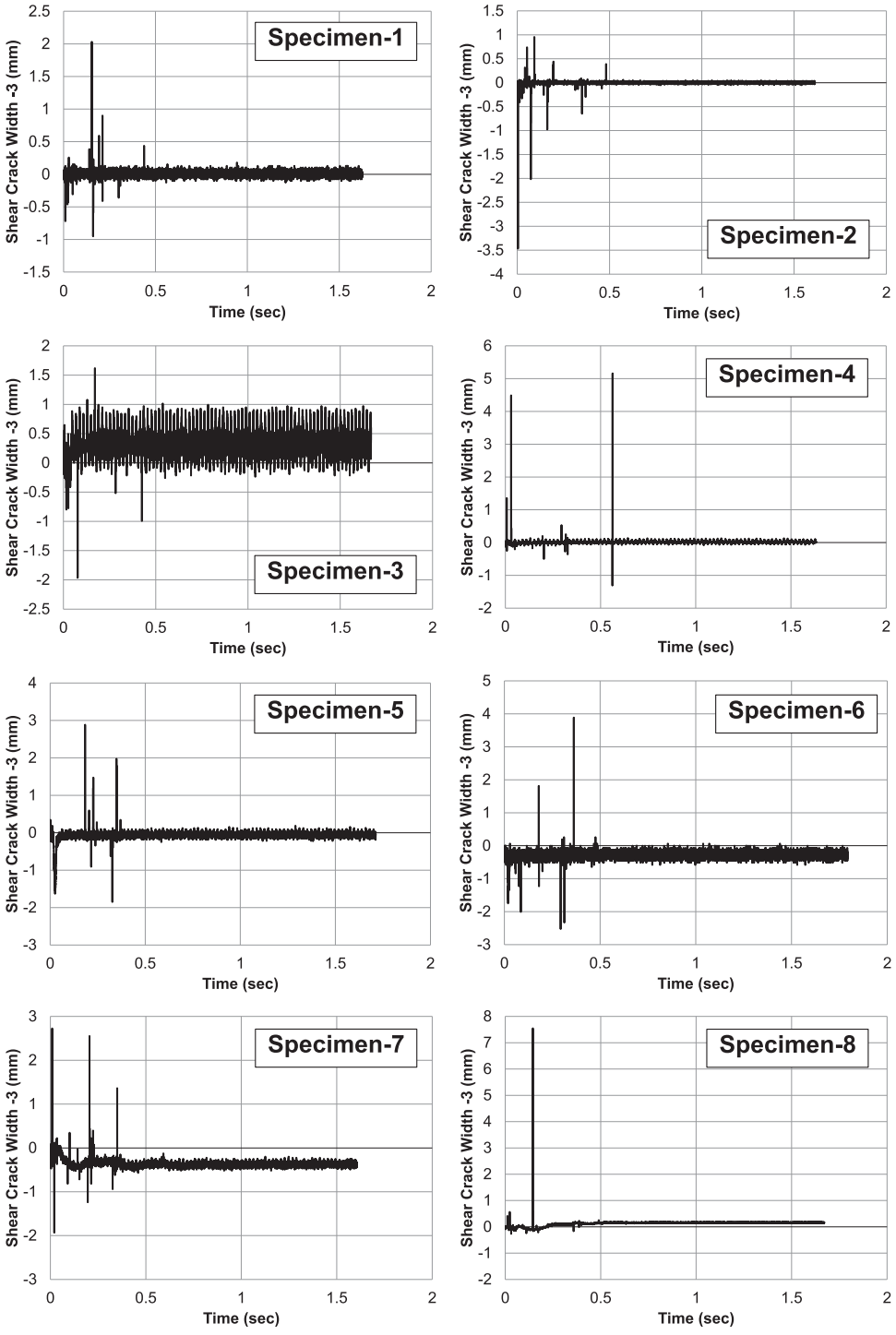

FIGURE 10 Shear crack width 3-time graphs of specimens

Under the effect of impact loading applied to test specimens, the maximum strain values were measured, on average, as 0.00854 and 0.01424 mm/mm for test specimen strengthening using CFRP with the spacing of 150 and 250 mm, respectively. These strain values are 71% and 158% greater than 0.005 mm/mm on average, respectively. The strain values measured from CFRP strips under the effect of sudden dynamic impact loading are much higher than the peel limit strain value of 0.005 mm/mm, which is defined for the peeling of the CFRP strips effect static loads presented in the ACI 440 Committee report.[53] This result has shown that the increase in material strength values with the effect of strain rate observed in other material types under dynamic loading is also valid for the interface of concrete and CFRP strips. This result demonstrates that the CFRP strips exhibit 2.3 times greater strain values in impulsive dynamic loadings according to static loadings. With this

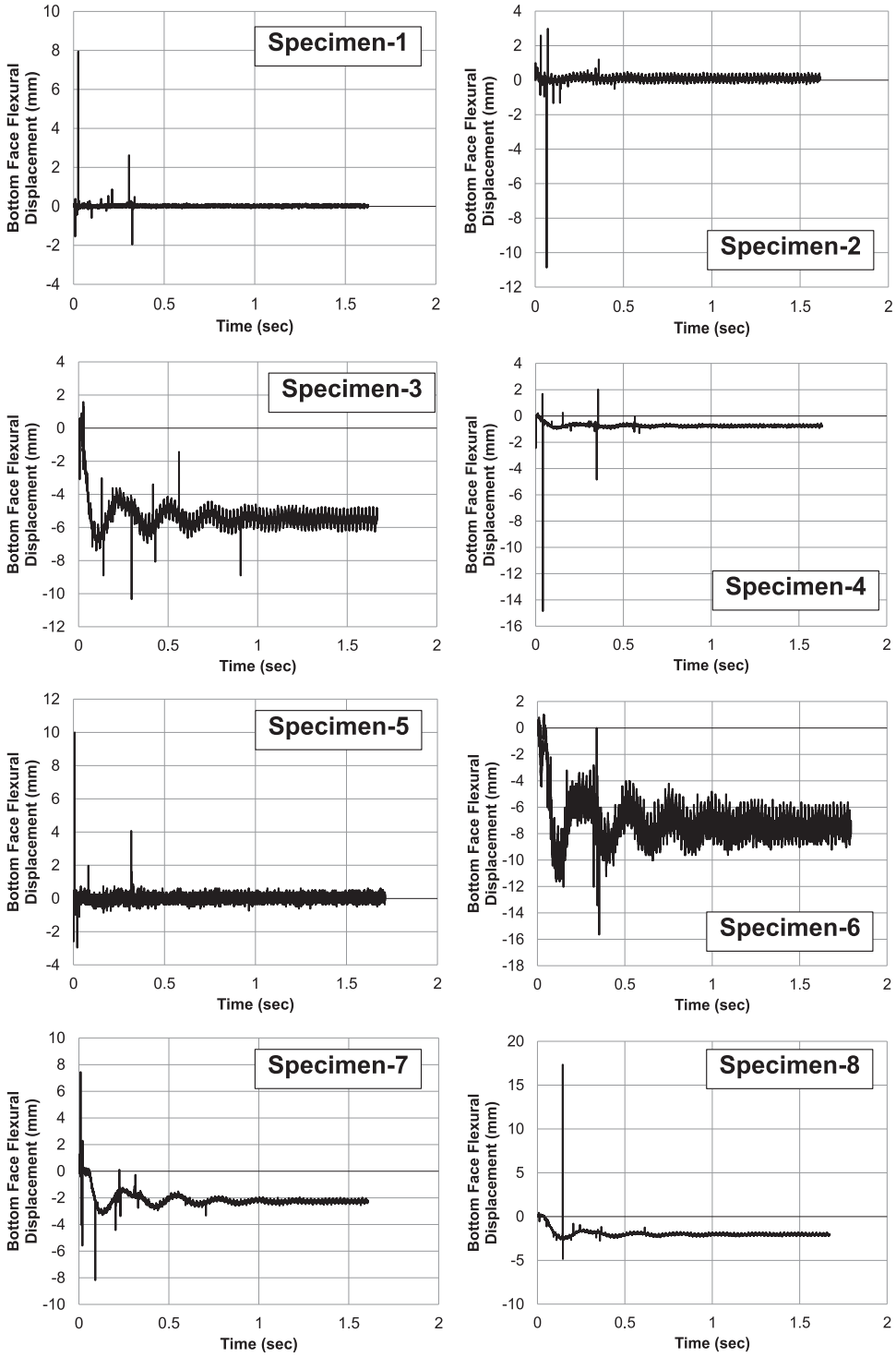

FIGURE 11 Bottom face flexural crack width–time graphs of specimens

result obtained, it is considered that strengthening of RC structures with CFRP against the impulsive dynamic effects becomes a good and utmost applicable alternative among the strengthening methods.

The second variable in the experiments is shear reinforcement spacing in the beam sections of the beam to column connection test specimens. Beam sections included shear reinforcement with the spacing of 300 mm or no shear reinforcement. Test specimens whose beam parts have shear reinforcements with the spacing of 300 mm exhibited, on average, 33% lower maximum acceleration values measured from beam-ends than test specimens whose beam parts have not shear reinforcements. Maximum shear crack width, maximum bending crack width, and residual beam end displacement values measured from the specimens without shear reinforcement were obtained 19%, 22%, and 26% greater than the specimens with shear reinforcement 300 mm

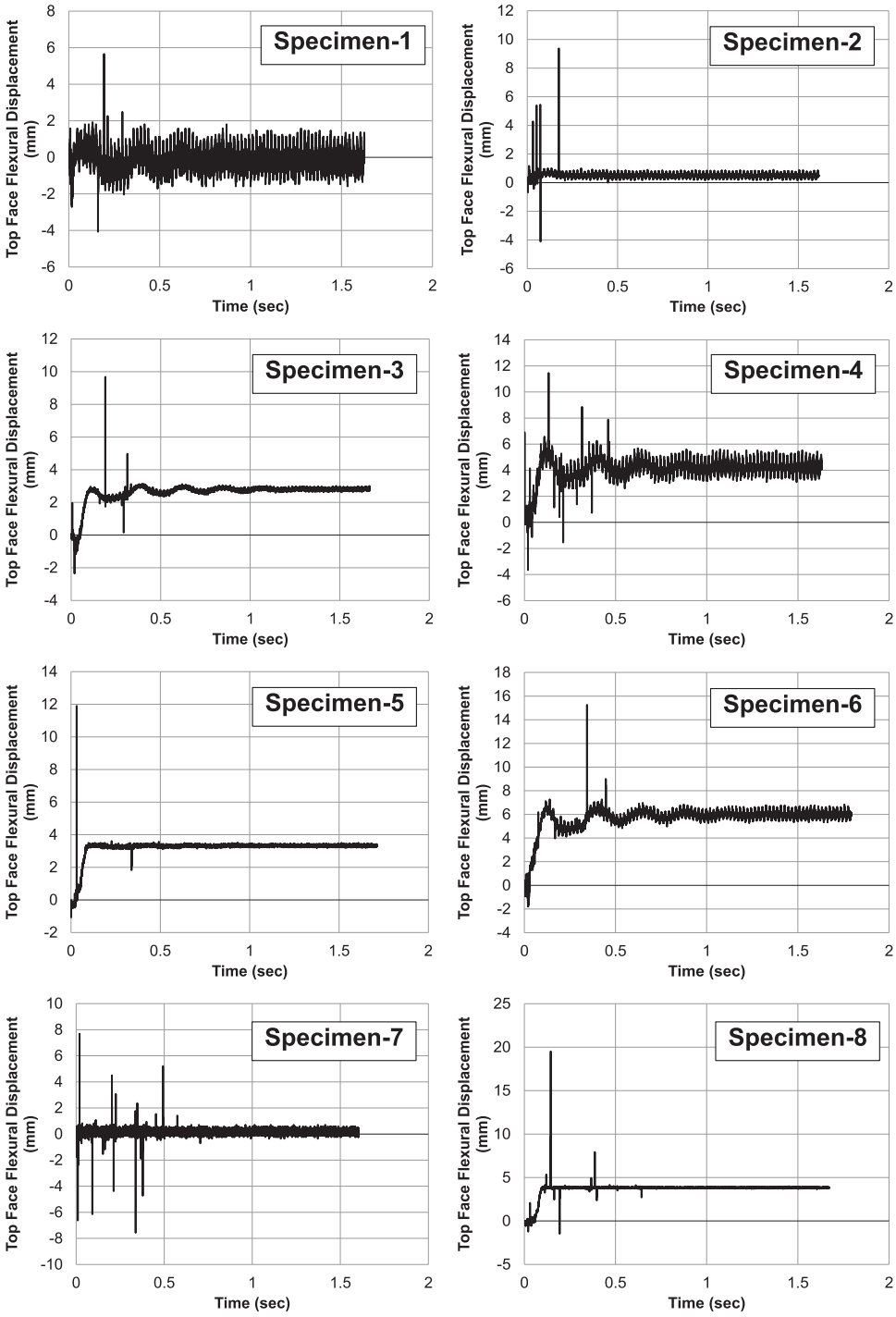

FIGURE 12 Top face flexural crack width–time graphs of specimens

spacings on average, respectively. Besides, maximum strain values measured from test specimens without shear reinforcement were obtained 34% greater than the specimens with shear reinforcement at 300 mm spacings on average, respectively. These results showed that the decrease of the shear reinforcement ratio in beam parts negatively affects performance and causes the increment of all of the maximum acceleration values, the displacement, and crack width values at the beam-column connections. The decrease of shear reinforcement ratio caused CFRP strips to be forced by reaching greater strain values and greater shear force. The increase of shear reinforcement spacing caused the increments of the number and the width of the shear cracks occurring in addition to the flexural cracks (Figure 14). Under the impact loadings with the same impact energy, the fact that shear fracture becomes dominant in the RC beam's failure mode to column connection led to more damage to test specimens. It absorbed more energy from the test specimen. The increase of the shear damages and the increase of

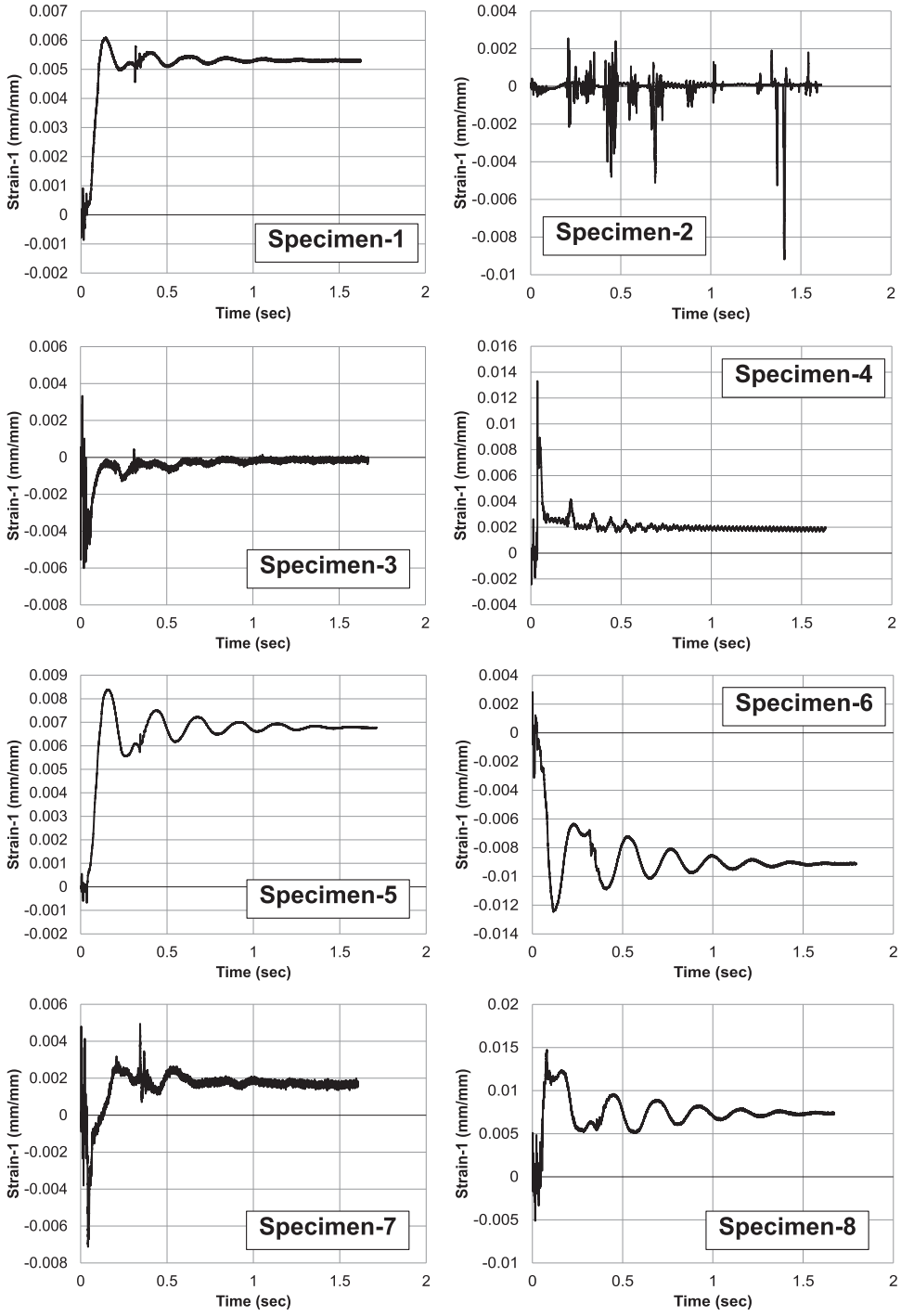

FIGURE 13 Maximum strain–time graphs of specimens

the energy transferred to test specimens increased the acceleration and displacement values measured from the RC beam to column connection specimens. These effects of the shear reinforcement ratio on the impact behavior of the RC beam to column connection specimens have been in good agreement with the results obtained from a considerable number of the experimental and analytical studies in the literature.[10,11,13,15,20,35,54–57]

The third variable investigated is the concrete compressive strength used for manufacturing beam to column connection test specimen. Test specimens have been manufactured in two different concrete classes, of which compressive strengths are 10 and 25 MPa. The increase of concrete compressive strength from 10 to 25 MPa increased the maximum acceleration values measured from beam ends, on average, 34%. However, this increment in concrete compressive strength led to the decrements of all displacements and crack widths. The maximum displacement and the maximum residual displacement at the beam end, the maximum shear crack width, and the maximum flexural crack width values decreased, on average, like 22%, 26%, 23%, and 22%.

TABLE 3 Experimental results

Spec. no	Beam tip acceleration (g)		Beam tip displacement (mm)	Maximum shear crack widths (mm)			Maximum curvature disp. (mm)		Residual beam tip displacement (mm)	Impact force (kN)	Maximum strain at CFRP strips (mm/mm)
	Maximum	Minimum		Beam-column joint	First	Second	Bottom	Top			
1	275.48	−58.52	22.84	1.32	3.84	2.98	9.90	9.73	15.87	6.57	0.00697
2	237.48	−46.60	31.29	1.87	5.42	4.42	13.85	13.49	21.63	6.51	0.01175
3	363.92	−186.21	27.43	1.58	4.57	3.59	11.92	12.03	18.59	6.51	0.00935
4	314.74	−67.01	37.86	2.44	6.58	6.47	16.87	15.11	26.84	6.49	0.01576
5	357.27	−131.43	31.32	1.72	5.03	4.74	12.96	12.98	17.88	10.01	0.00908
6	313.41	−72.42	40.69	2.75	7.20	6.42	16.65	17.06	32.76	10.05	0.01529
7	481.13	−414.68	35.96	2.01	5.93	4.66	15.63	15.26	23.99	10.06	0.01208
8	412.98	−150.71	49.04	3.19	8.55	7.82	22.19	20.99	33.40	10.08	0.01983
9	372.20	−246.49	18.26	1.05	3.08	2.38	7.89	7.92	10.97	6.51	0.00559
10	326.60	−165.51	25.04	1.47	4.33	3.54	11.08	10.85	21.31	6.50	0.00938
11	493.73	−143.62	21.91	1.28	3.64	2.84	9.53	9.62	15.42	6.53	0.00748
12	423.39	−334.14	30.29	1.96	5.25	5.17	13.50	12.11	22.02	6.49	0.01261
13	483.99	−381.19	25.54	1.42	4.16	3.21	10.65	10.70	15.45	10.01	0.00756
14	418.04	−137.60	34.98	1.99	5.84	4.76	14.96	14.65	19.28	10.00	0.01228
15	628.60	−380.89	30.61	1.73	4.91	3.83	12.87	12.97	18.48	10.01	0.01023
16	536.76	−450.31	41.99	2.62	7.07	6.97	18.20	16.34	32.73	10.00	0.01702

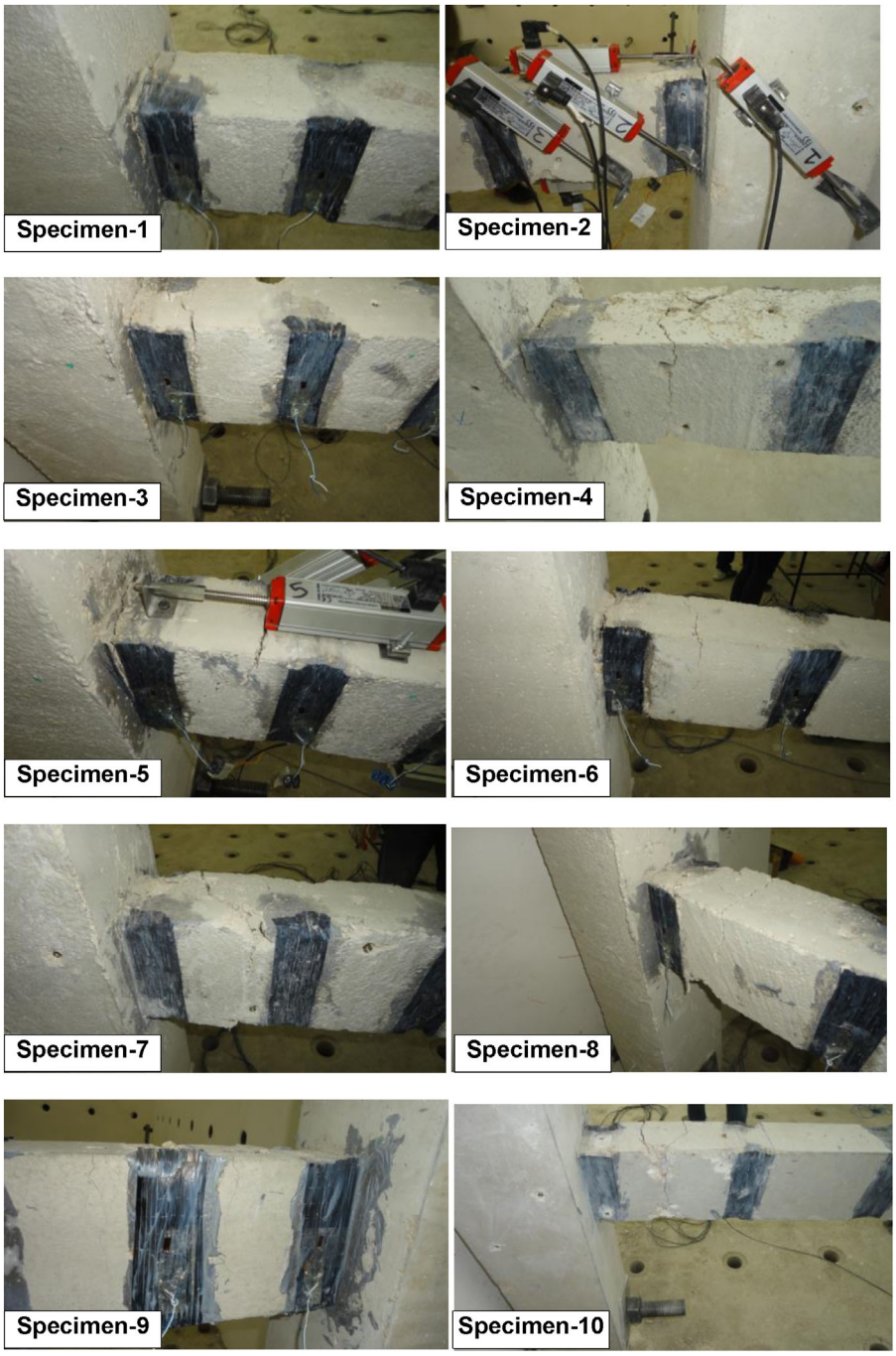

FIGURE 14 Crack distribution of test specimens after test

Besides, the maximum strain values measured from CFRP strips decreased, on average, 22% with the increase of the concrete compressive strength. It is observed that the maximum acceleration values of the specimens manufactured from a lower strength concrete (10 MPa) were subjected to lower acceleration magnitudes. Lower strength concrete may be attributed to the lower stiffness and related energy dissipation capacity of the specimens manufactured using a lower strength concrete (10 MPa). The results obtained from this study are in good agreement with similar studies in the literature. According to the literature studies, an increase in the compressive strength of concrete leads to an increase in the measured

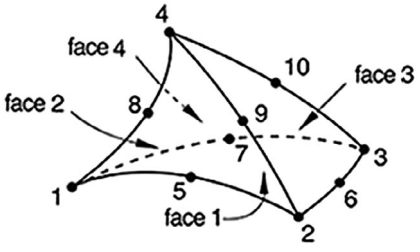

FIGURE 15 Element type in the analysis

acceleration values, generally. The increase of concrete compressive strength leads to an increase in the toughness of elements. This increment in toughness also increased the

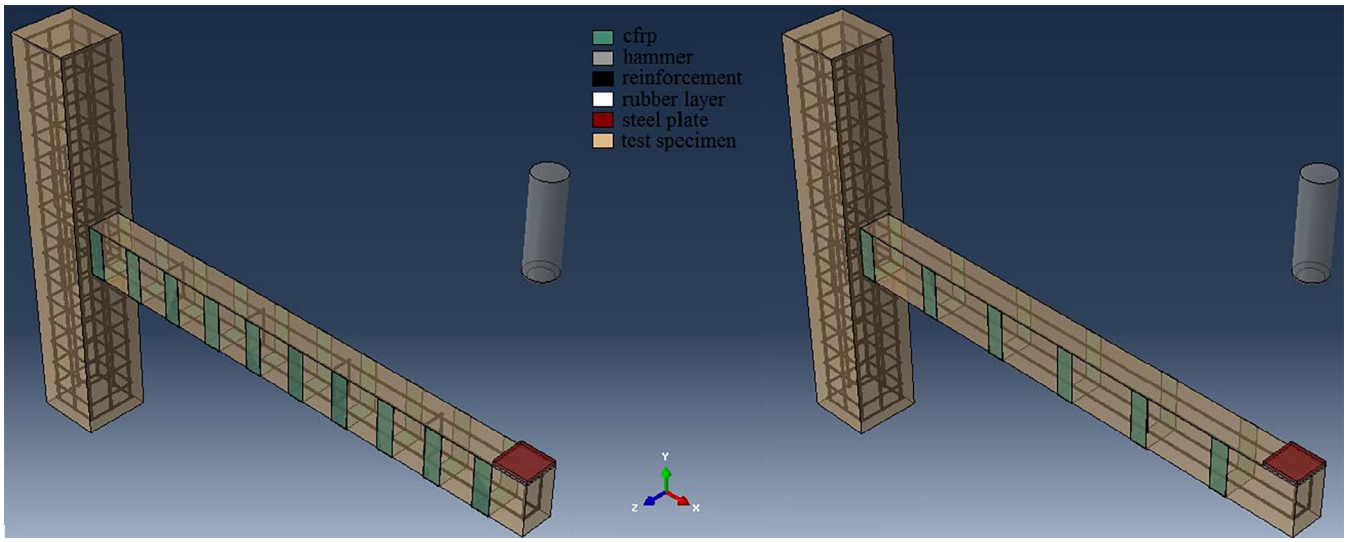

FIGURE 16 Finite element models

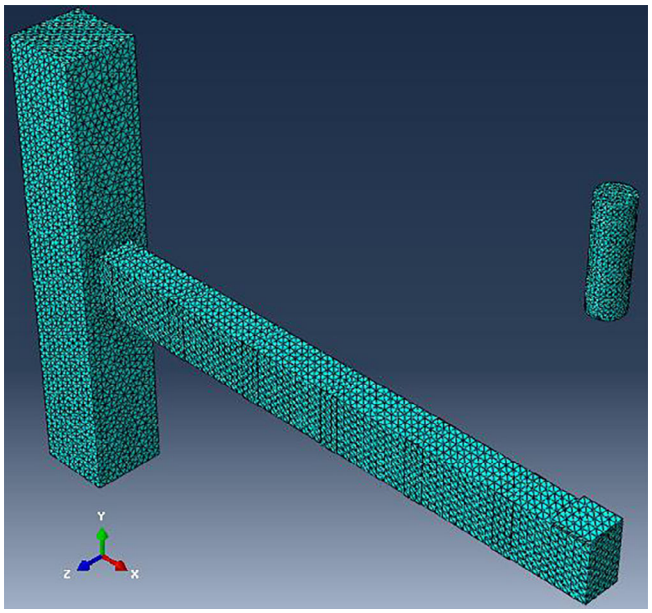

FIGURE 17 Specimen 2 after mesh operation

test specimens' acceleration values subjected to impact loading conditions with identical energy levels. These results implied that the impact load and the energy capacity of structural members manufactured using normal strength concrete (25 MPa) are higher than their counterparts manufactured using low strength concrete (10 MPa). Low level of acceleration magnitudes measured from elements manufactured using low strength concrete (10 MPa) showed that they absorbed a low level of impact energy. An increase in the compressive strength of concrete used in the test specimens improved the general impact behavior. Similar results are also observed in the study of Liao et al.[58] Results obtained demonstrated that the increase of the concrete compressive strength improved test specimens' impact performance and the accelerations have increased, whereas the displacements have decreased. Furthermore, the concrete compressive strength increase decreased the strain values measured from CFRP strips and provided lower shear force acts on CFRP strips.

The last variable investigated in the experimental study's scope is input impact energy transmitted to test specimens. Two different level input impact energies were applied to test specimens by dropping steel hammer with constant weight from two different drop-heights are 500 and 750 mm. The increase of input impact energy increased maximum acceleration, maximum displacement at beam end, maximum shear crack width, maximum flexural crack width, maximum residual displacement at beam end, and maximum strain values like 30%, 36%, 33%, 32%, 27%, and 32%. The maximum contact force was determined as 6.51 kN when the test specimen had been subjected to impact loading with an impact energy of 0.4120 kJ. The maximum force acting on test specimens increased to 10.01 kN when impact loading with the impact energy of 0.6190 kJ had been applied. The increase of input energy performed by dropping steel hammer from 750 mm height instead of 500 mm increased the maximum contact force transferring to the test specimens by 54%. The increase of the contact force increased all acceleration, displacement, and strain values. The photos illustrating the crack patterns and damages due to impact loading were presented in Figure 14. When Figure 14 is analyzed, it can be seen that the crack pattern and damages are accordant with the displacement measurements taken from the beam to column connection test specimens. When the distribution of damage that occurred in the specimens was examined, it was

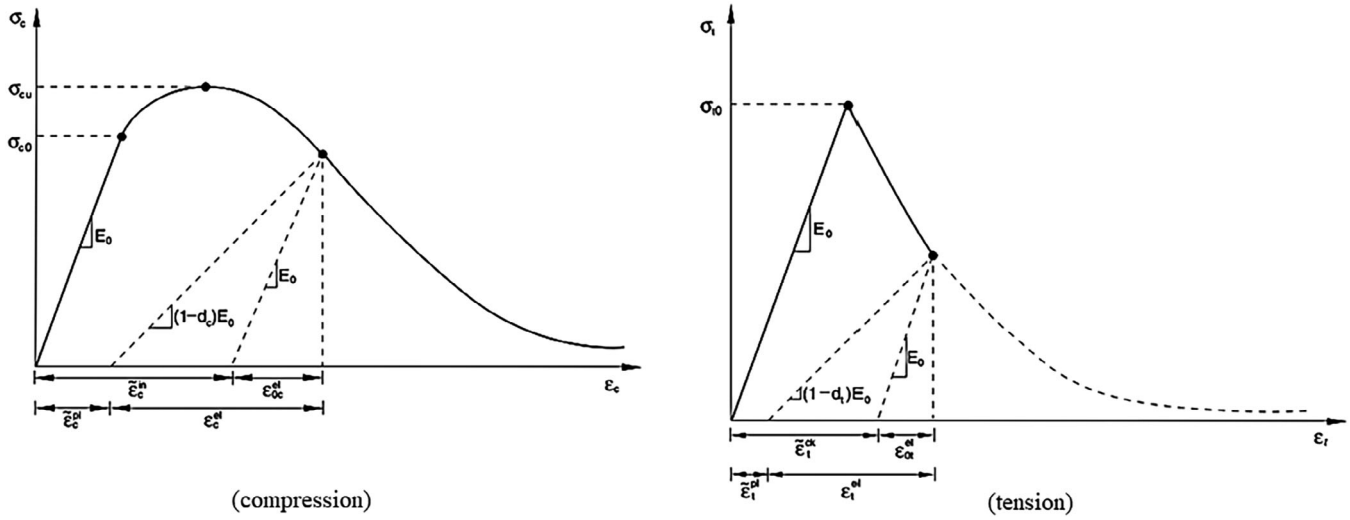

FIGURE 18 Material model of concrete

TABLE 4 Mechanical properties of concrete

Property	Values for C10	Values for C25
Poisson's ratio	0.20	
Density (kg/m^3)	2400	
Modulus of elasticity (MPa)	14,862.70	23,500
Compressive strength (MPa)	10	25
Tensile strength (MPa)	1.97	3.11
ψ	30	
e	0.10	
σ_{b0}/σ_{c0}	1.16	
K_c	0.6667	
μ	0.0001	

seen that the specimen with the most damage was Specimen 8. Beam tip displacement, shear crack widths, and bending crack widths measured from Specimen 8 are the largest experimental program values. It was observed that the concrete was crushed due to the impact loading in the lower pressure zone of the beam of Specimen 8, and spalling occurred in the concrete shell. Furthermore, when the crack patterns that occurred in test specimens are analyzed, it can be concluded that the strengthening with CFRP strips has been successful at limiting and decreasing crack widths for the shear-deficient test specimens. Test specimens strengthening using CFRP with the spacing of 150 mm have less damaged, exhibited lower beam-end displacements and crack widths than test specimens strengthening using CFRP with 300 mm. The decrease of shear reinforcement ratio and the increase of applied input impact energy led to more damage and enhanced crack widths. However, the increase of the concrete compressive strength limited damages and decreased the crack widths.

4 | NUMERICAL ANALYSIS

In the numerical analysis part of the study, finite element models of test specimens have been generated by ABAQUS software (ABAQUS Users' Manual, 2015). In parallel with this purpose, the software's explicit module is utilized to verify test results obtained from the experimental program. This module manages to perform nonlinear incremental analysis via many advanced material models. Researchers and engineers investigate structural members' behavior under sudden impact effects by ABAQUS/Explicit in recent years.

The numerical analysis's first step is creating three-dimensional finite element models of the test specimens, hammer, loading plate, longitudinal and transverse steel bars, CFRP strips, and test setup in the software. C3D10M (10 nodes modified tetrahedron) shaped elements that give the most accurate results for such problems are used in the modeling phase of the finite element models (Figure 15).[49] Finite element models of Specimens 1 and 4 are presented in Figure 16 to show two different reinforcement configurations. Support conditions of test specimens are provided in the software. For this purpose, support regions of the specimens are defined with the boundary conditions with the same boundary conditions in the experimental study in horizontal, vertical, and axial directions. A steel hammer applies impact loading on the specimens. So, the movement of the

TABLE 5 Material characteristics of steel and rubber

Property	Steel bars with 8 mm	Steel bars with 4 mm	Hammer and plate	Rubber
Poisson's ratio	0.30	0.30	0.30	0.45
Density (kg/m^3)	7850	7850	7850	1230
Young's modulus (MPa)	209,000	210,000	200,000	22
Shear modulus (MPa)	80,384.61	80,769.23	76,923.08	7.59
Bulk modulus (MPa)	174,166.67	175,000	166,670	73.33
Yield strength (MPa)	485	415	–	–

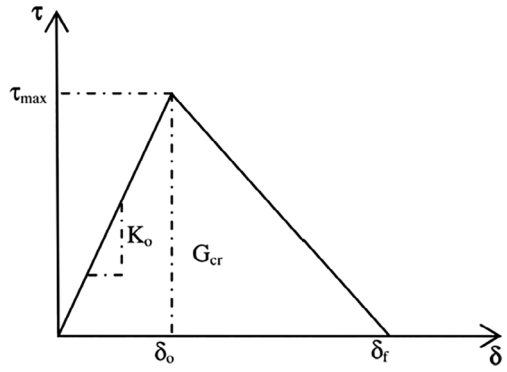

FIGURE 19 Bilinear traction–constitutive separation law

hammer in the vertical direction is released in the analysis. Because the problem is a free-fall test, the only gravity force is assigned to the hammer. After generating finite element models with boundary conditions, mesh operation has been performed in the software. The mesh structure of the models is provided by considering the element and analysis types. For this purpose, comparative and sensitivity analysis between 10 and 25 mm is performed to reach the most convenient finite element size. As test specimens include steel bars and CFRP strips, computation time extends when smaller values are used in the analysis. So, the finite-element size is decided as 20 mm for all models. This study used 1, 242,220 nodes and 174,197 elements for Specimen 1, 233,842 nodes and 168,322 elements for Specimen 2, 236,684 nodes and 169,919 elements for Specimen 3 and 230,816 nodes and 165,948 elements for Specimen 4, respectively. The finite element model of Specimen 2 is shown after mesh operation in Figure 17.

Material characteristics of concrete, steel bars, loading plate, hammer, and CFRP strips are defined and assigned to related geometries in the software before performing numerical analysis. The concrete damage plasticity model, a continuum, plasticity-based, damage model is used to define the non-linear property of concrete in the software. In this way, concrete behavior is successfully determined by providing a stress–strain relationship in compression and tension regions, as presented in Figure 18. The concrete damage plasticity model is the best way to define the complex behavior of concrete. In the compression region, a linear response is obtained until the initial yield value, σ_{c0}. However, the behavior of concrete is different in the plastic zone. In this part, the response is determined by the stress hardening followed by strain-softening beyond the value of ultimate stress, σ_{cu}. In the tension region, linear elastic behavior is obtained until reaching failure stress value, σ_{t0}. Microcracks in concrete occur beyond this point in the stress–strain relationship. The formation of these micro cracks is characterized by softening stress–strain response after failure stress. There are two damage variables as d_t and d_c in the concrete damaged plasticity model. These variables are utilized for elastic stiffness degradation. The values of the damage variables change between $0 < d_t$ and $d_c < 1$. Undamaged material is represented by zero. On the other hand, total loss of strength is represented by one. Stress–strain relationships under the effect of tension and compression loading are obtained by Equations (1) and (2). Parameters such as E_0, $\tilde{\varepsilon}_t^{pl}$ and $\tilde{\varepsilon}_c^{pl}$ are the material's initial elastic stiffness, the equivalent plastic strain in tension, and compression in the equations below.[59]

$$\sigma_t = (1 - d_t)E_0\left(\varepsilon_t - \tilde{\varepsilon}_t^{pl}\right) \quad (1)$$

$$\sigma_c = (1 - d_c)E_0\left(\varepsilon_c - \tilde{\varepsilon}_c^{pl}\right) \quad (2)$$

The concrete damage plasticity model is based on five different parameters. These parameters are used to define the yield surface function, the potential flow, the material's viscosity, and the compressive and tensile behavior of concrete in concrete, damaged plasticity model. These parameters are dilation angle, the flow potential eccentricity, the ratio of initial equibiaxial compressive yield stress to initial uniaxial compressive yield stress, the coefficient determining the shape of the deviatoric cross-

TABLE 6 Comparison of experimental and numerical results

	Acceleration (g)					Displacement (mm)			Impact load (kN)		
	Experimental		Numerical								
Specimen no	Max	Min	Max	Min	Ratio[a]	Experimental	Numerical	Ratio[b]	Experimental	Numerical	Ratio[c]
1	275.48	−58.52	281.43	−262.59	0.98	22.84	23.85	0.96	6.57	7.46	0.88
2	237.48	−46.60	259.52	−243.74	0.92	31.29	27.46	1.14	6.51	7.65	0.85
3	363.92	−186.21	310.37	−321.86	1.17	27.43	27.63	0.99	6.51	8.01	0.81
4	314.74	−67.01	307.16	−258.53	1.02	37.86	31.72	1.19	6.49	8.24	0.79
5	357.27	−131.43	345.44	−314.61	1.03	31.32	32.07	0.98	10.01	11.88	0.84
6	313.41	−72.42	327.81	−302.48	0.96	40.69	35.63	1.14	10.05	12.07	0.83
7	481.13	−414.68	417.68	−435.37	1.15	35.96	37.21	0.97	10.06	12.16	0.83
8	412.98	−150.71	385.92	−357.54	1.07	49.04	40.72	1.20	10.08	12.38	0.81
9	372.20	−246.49	386.35	−331.56	0.96	18.26	19.28	0.95	6.51	8.13	0.80
10	326.60	−165.51	357.48	−318.23	0.91	25.04	21.63	1.16	6.50	8.22	0.79
11	493.73	−143.62	437.26	−364.83	1.13	21.91	23.13	0.95	6.53	8.57	0.76
12	423.39	−334.14	388.17	−392.54	1.09	30.29	26.51	1.14	6.49	8.74	0.74
13	483.99	−381.19	442.73	−452.35	1.09	25.54	27.38	0.93	10.01	12.35	0.81
14	418.04	−137.60	439.64	406.17	0.95	34.98	31.74	1.10	10.00	12.64	0.79
15	628.60	−380.89	558.36	−485.27	1.13	30.61	33.16	0.92	10.01	12.59	0.80
16	536.76	−450.31	478.52	−486.44	1.12	41.99	35.67	1.18	10.00	13.08	0.76
Average					1.04			1.06			0.81
COV					7326.48			43.17			3.74

[a]Ratio of experimental maximum acceleration values to numerical results.
[b]Ratio of experimental displacement values to numerical results.
[c]Ratio of experimental impact load values to numerical results.

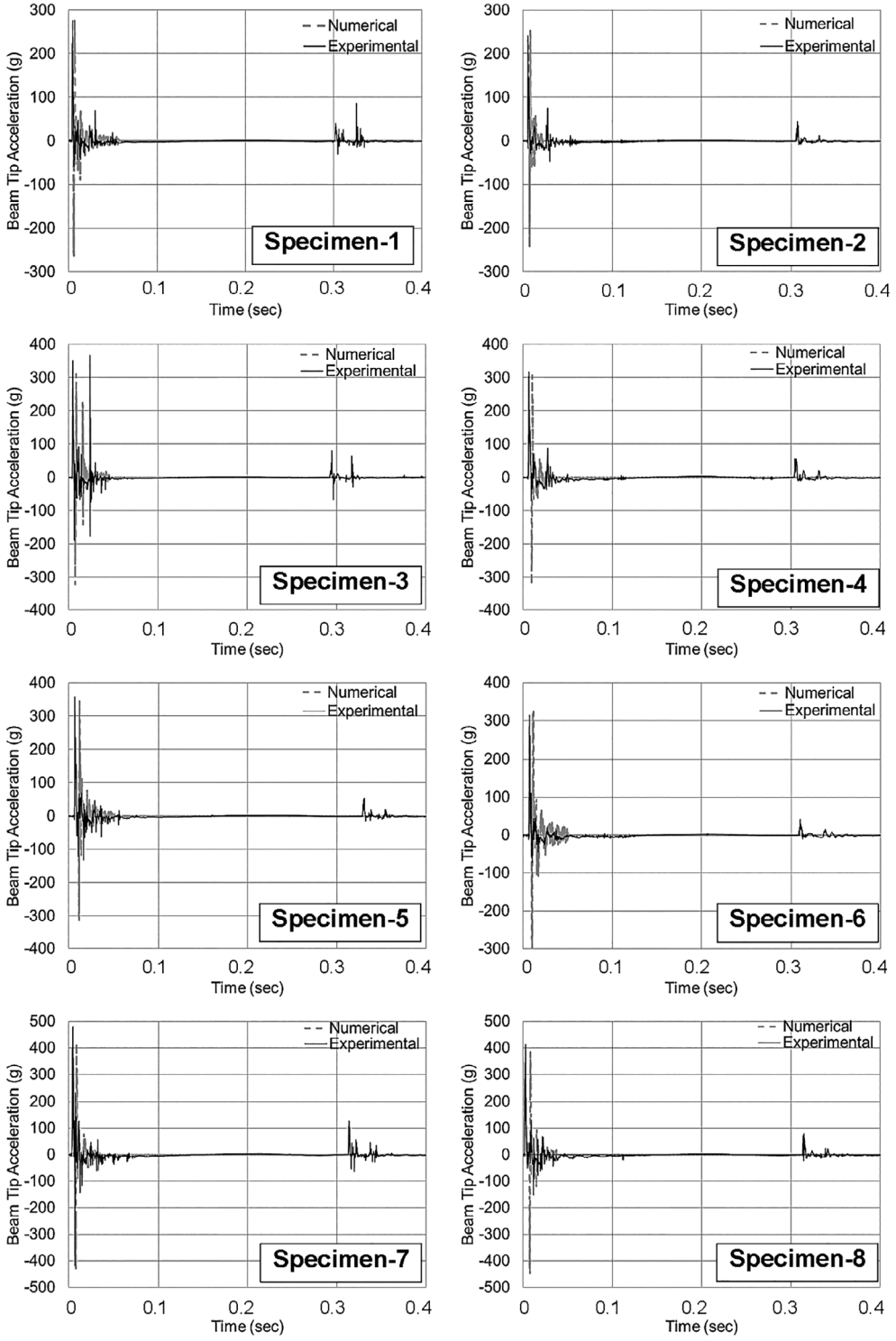

FIGURE 20 Comparison of acceleration–time graphs

section, and the viscosity parameter that is symbolized by (ψ), (e), (σ_{b0}/σ_{c0}), (K_c), and (μ), respectively. Other parameters of the concrete damage plasticity model are Young's modulus, Poisson's ratio, density, compressive, and tensile strengths.[37,49] All of these parameters have been defined in the software for two different concrete compressive strengths determined in the experimental part of the study. Mander's stress–strain model for unconfined concrete is utilized to define the behavior of concrete. Young's modulus of concrete (E_c) is calculated by considering the compressive strength value (f_c) as given in Equation (3).[60] On the other hand, the tensile strength

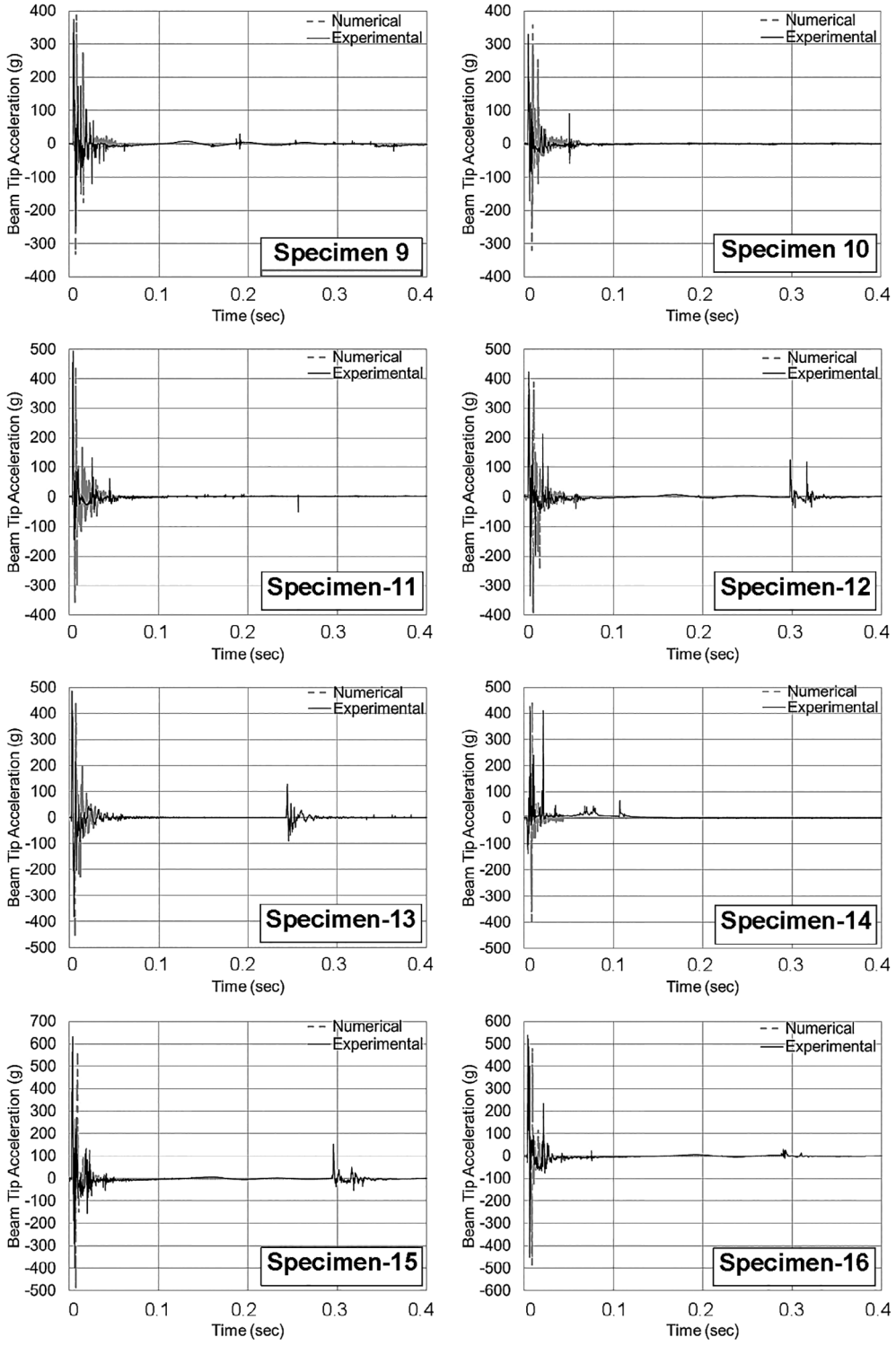

FIGURE 20 (Continued)

of concrete (f_t) is determined according to Equation (4). Besides, the ultimate concrete strain value (ε_{cu}) is taken as 0.003 in the software. Material properties of concrete are given in Table 4.

$$E_c = 4700\sqrt{f_c} \tag{3}$$

$$f_t = 0.623\sqrt{f_c} \tag{4}$$

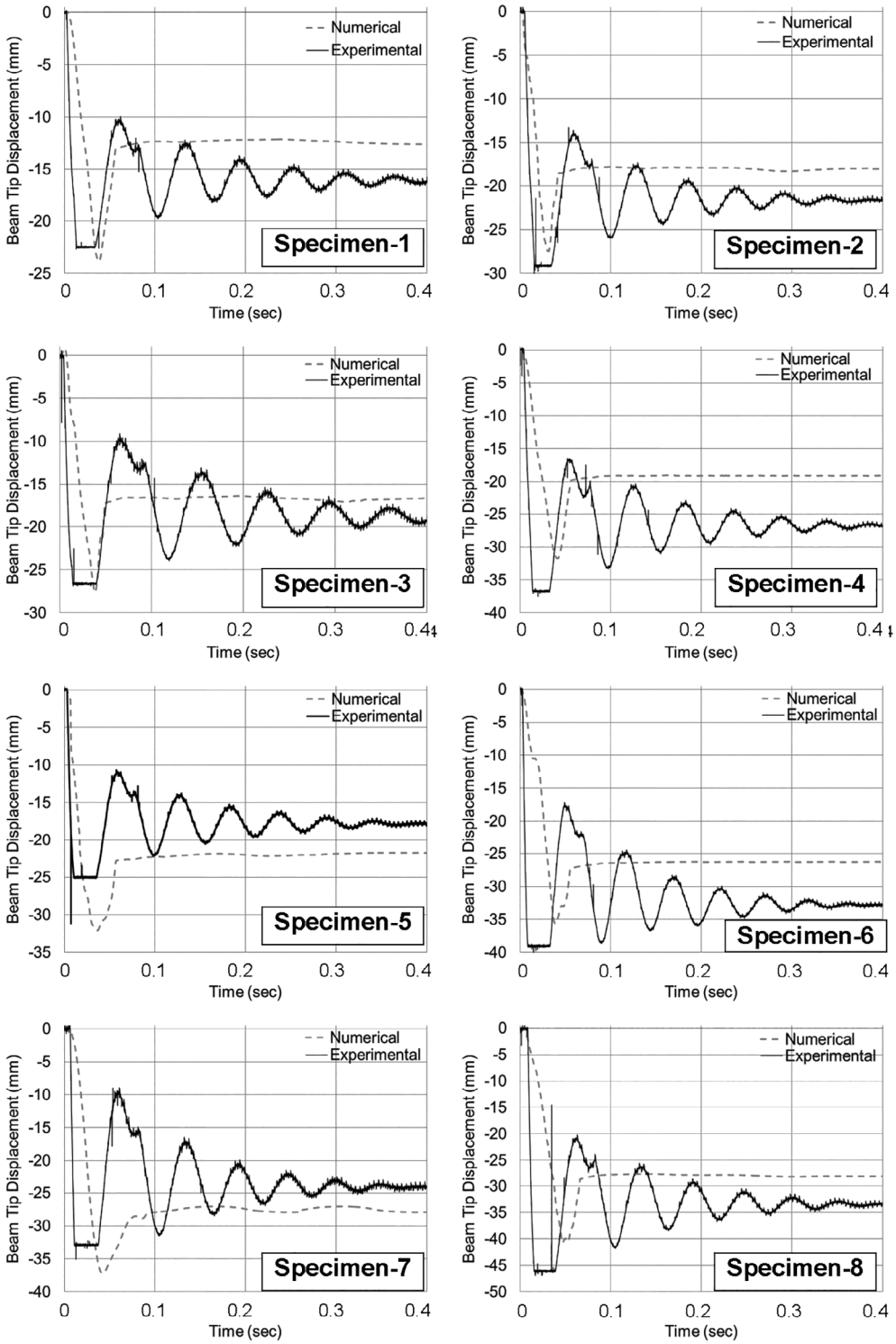

FIGURE 21 Comparison of displacement–time graphs

The tension and compression behavior of concrete material subjected to impact load is strain-rate dependent. The strength of concrete can be remarkably enhanced at high strain rates. Thus, the consideration of the strain rate effect gains importance to predict reliable dynamic response. The strain rate effect is commonly expressed by a dynamic increase factor (DIF) that is dynamic to static strength versus strain rate. Many empirical equations define the strain rate effect on concrete material for tension and compression behaviors.[61,62] These empirical DIF

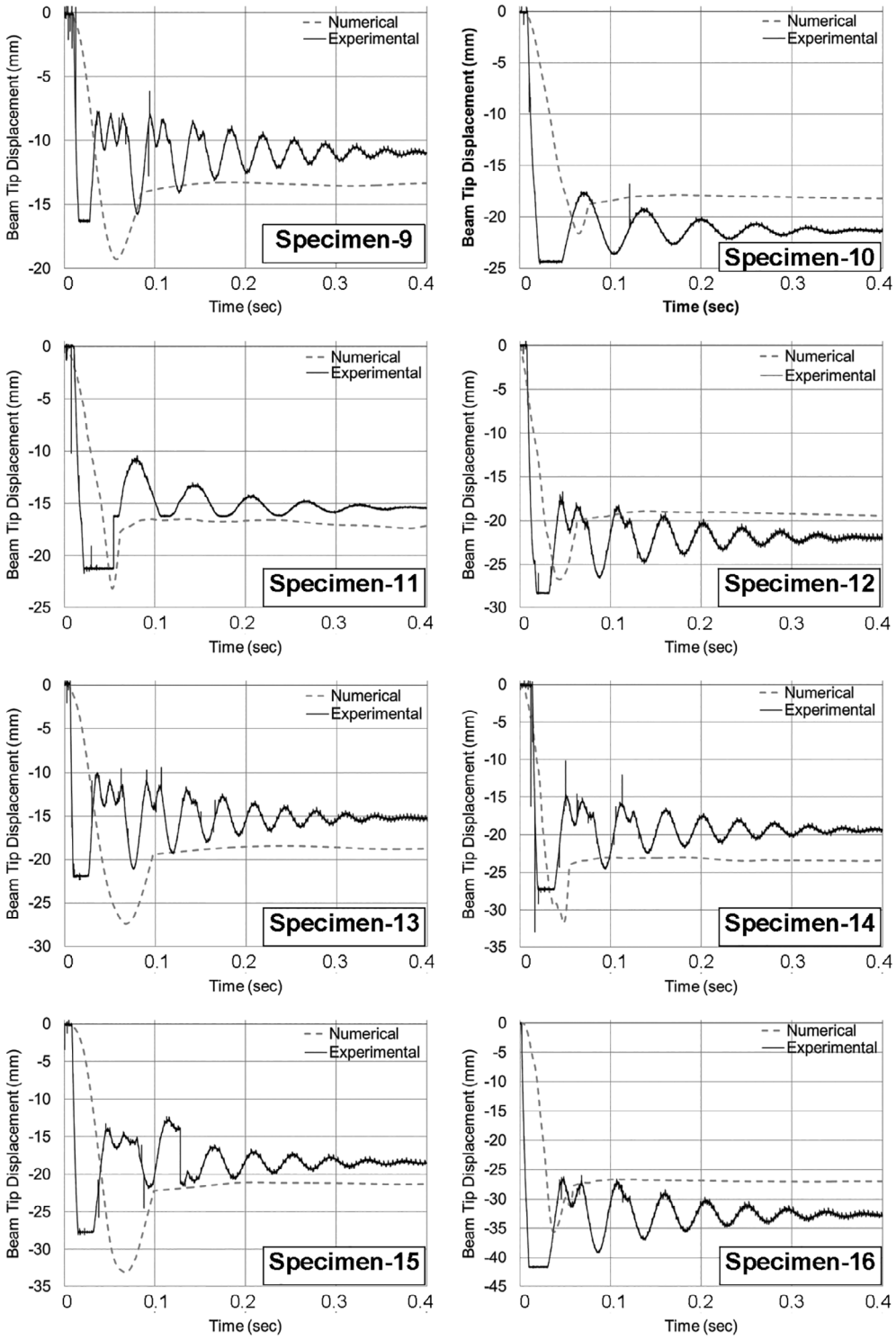

FIGURE 21 (Continued)

formulations can be easily implemented in concrete models in ANSYS and LS-DYNA software.[2,63,64] However, the CDP model cannot consider the rate-dependent behavior of concrete automatically. The user must provide different tension stiffening curves as a tabular function of cracking strain rate and several compression hardening curves as a tabular function of inelastic strain rate manually.[59] Besides, it is important to note here that this approach does not perfectly apply the strain rate effects on all aspects of concrete behavior.[65] However, in the previous study, a simplified iterative approach is proposed. The uniaxial curves are updating in each iteration

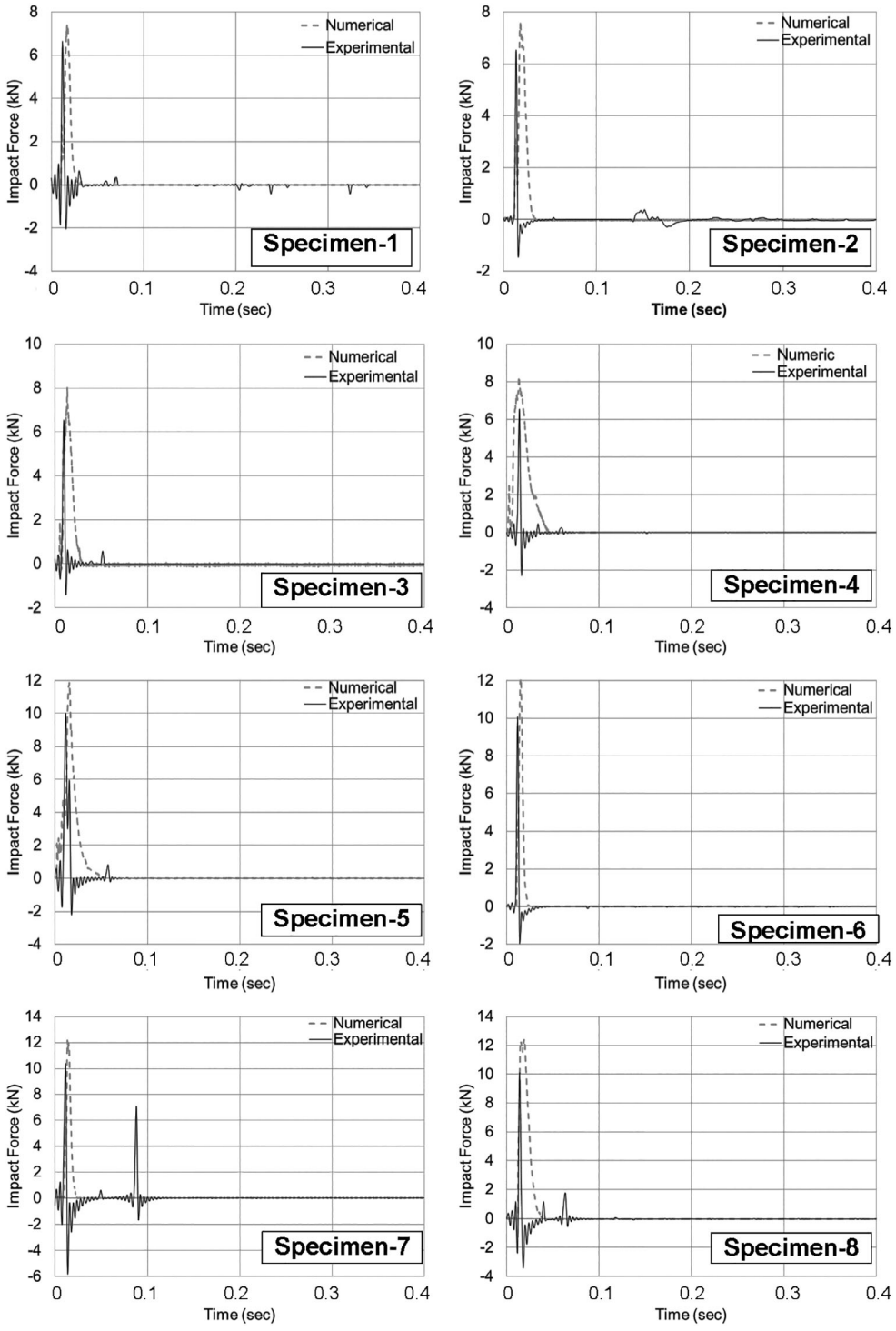

FIGURE 22 Comparison of impact load–time graphs

using DIF and the calculated strain rates obtained from the mid-span section until adequate convergence is achieved. However, it is expressed that this iterative approach gives reasonable results only up to the first peak of response while it is inadequate in represent a post-peak response. Therefore, the authors have decided that the strain rate effects in concrete are not included in the finite element model in this study's scope because the CDP model does not include an algorithm considering strain-rate effect automatically.

Linear elastic material models are used to define the steel bars' material characteristics, the loading plate, and the rubber in the software. Properties of steel bars are defined according to obtained results in the experimental

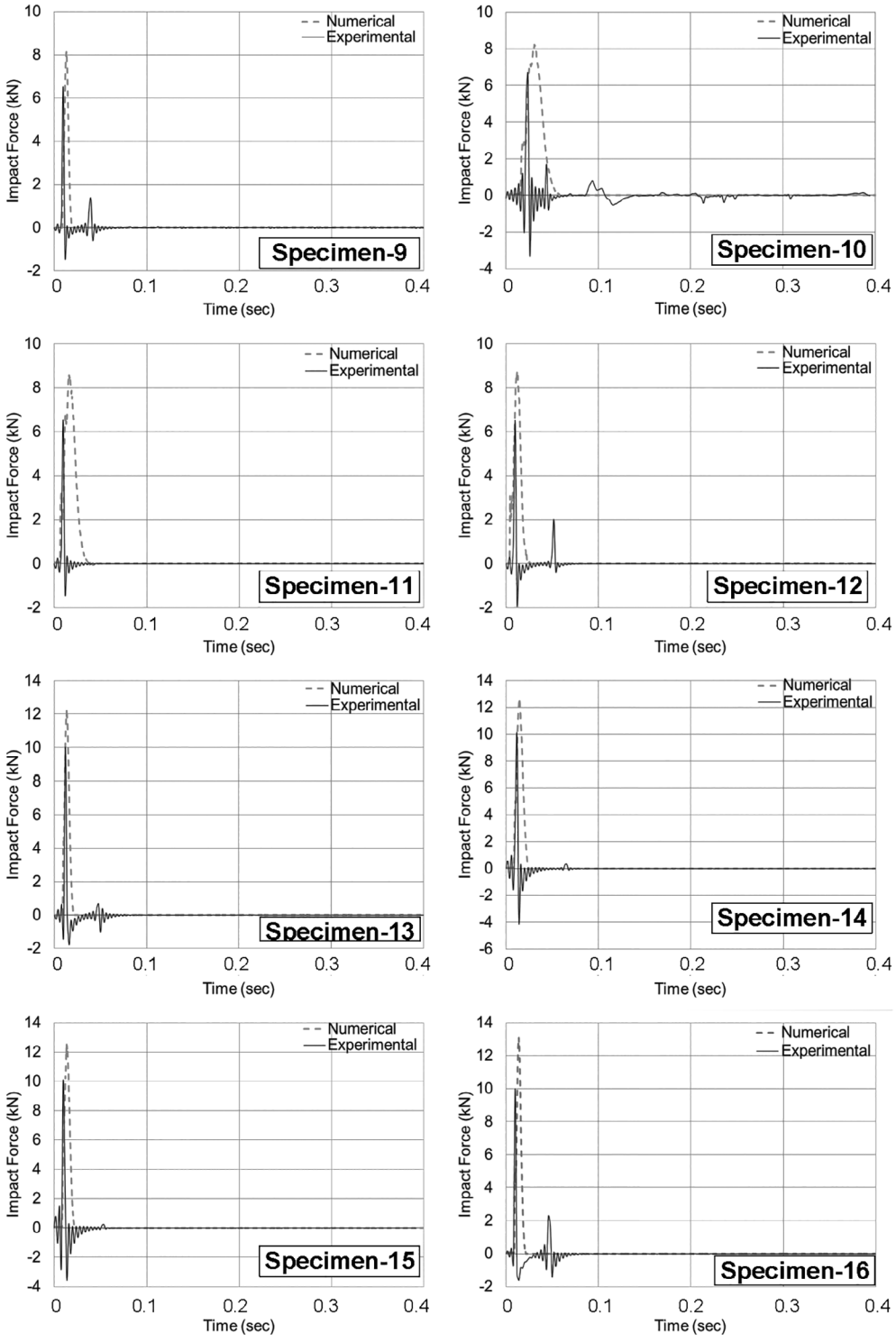

FIGURE 22 (Continued)

program. Yield strength, Young's modulus, Poisson's ratio, bulk modulus, and shear modulus values for steel and rubber are given in Table 5. Steel bars are embedded in test specimens. The tie contact property of the software is utilized to provide adherence between steel bars and the specimens.

After completing the concrete, steel, and rubber material characteristics, the CFRP strips' properties are defined in the software. For this purpose, the values in Table 2 obtained from the manufacturer are utilized for the related parts of the specimens. Besides, the cohesive zone model is used to define the interface between

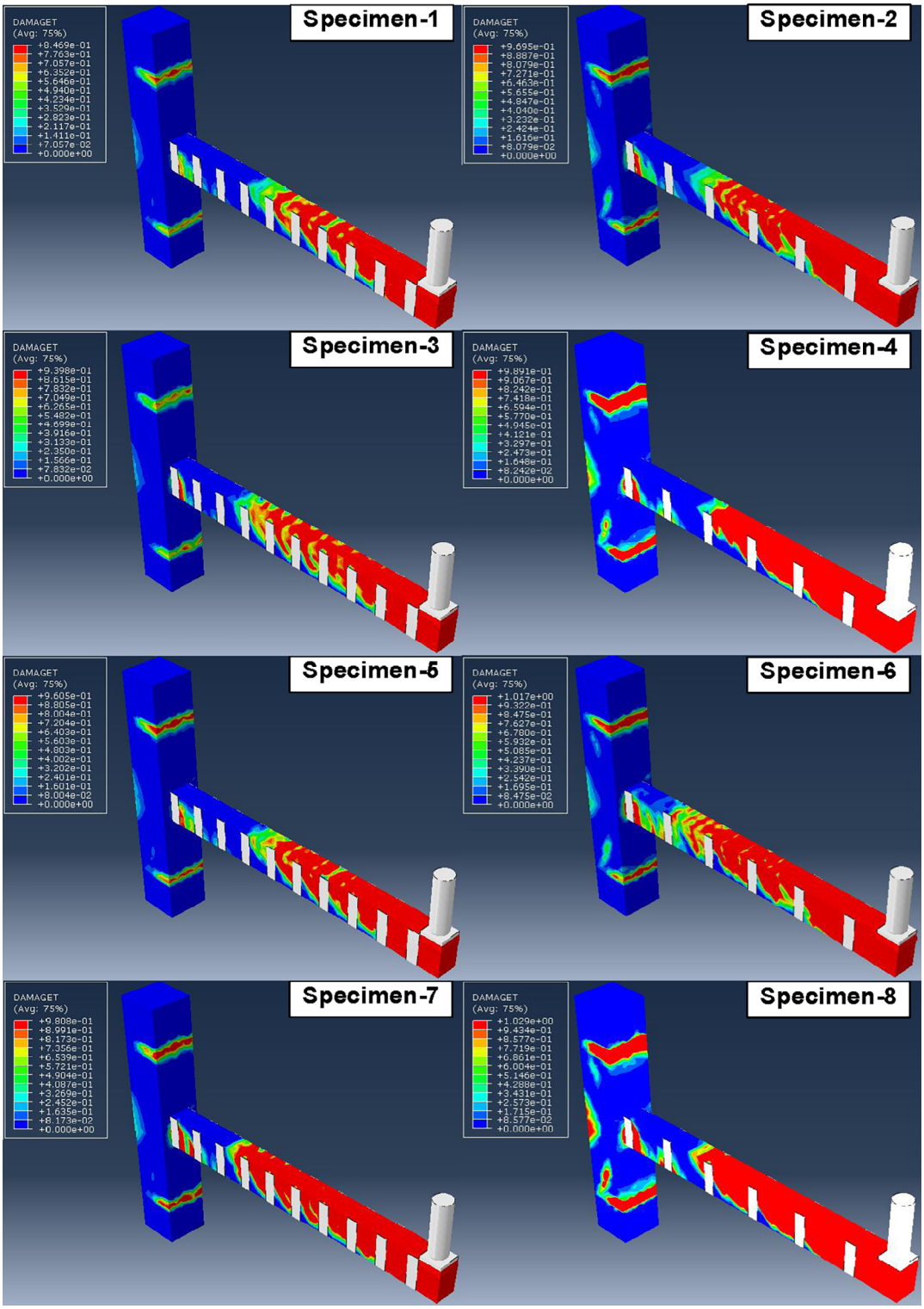

FIGURE 23 Damage patterns of the specimens

concrete and CFRP. This model is based on bilinear traction-separation law represented by effective traction τ, and effective opening displacement δ as presented in Figure 19. Stiffness is expressed by K_0, the local strength of the material is τ_{max}, opening displacement corresponding to fracture is δ_f, and the energy required for opening crack G_{cr} are used for the definition of τ–δ relationship in the figure.

The software's contact property is used to define the connection between the hammer and the test

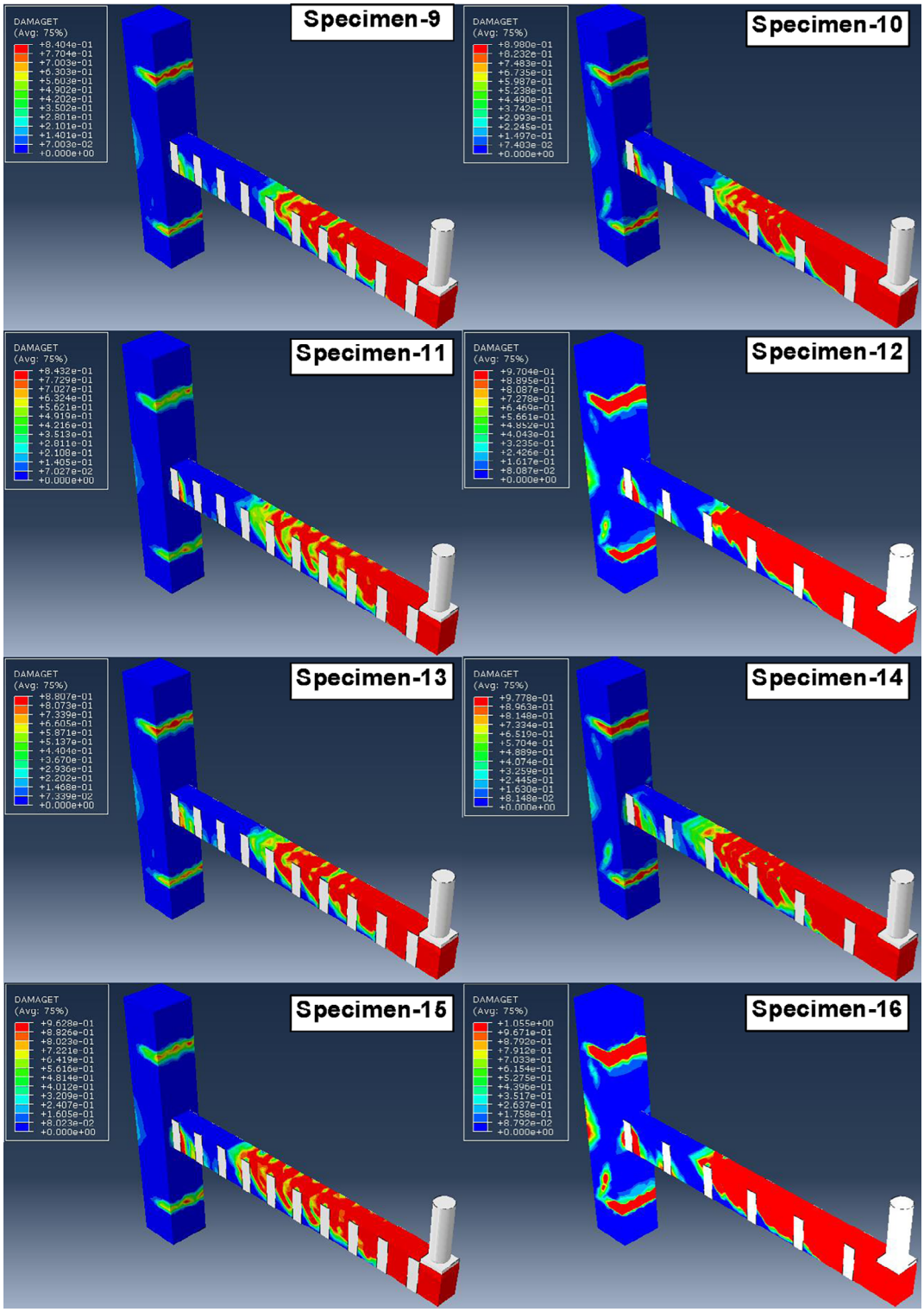

FIGURE 23 (Continued)

specimen. For this purpose, the surface to surface contact is utilized for the hammer and specimen surfaces. Since it is impossible to remove friction effects during the experimental program, the friction coefficient for contact surfaces is taken as 0.02 in tangential behavior. The hammer applies impact loading on the specimens. For this reason, the surface of the hammer is defined as the master in the numerical analysis. On the other hand, the surface of the specimen is defined as the slave. Another

important parameter of the numerical analysis is defining time increments and steps. Because incremental dynamic analysis is performed in the software, time increments and steps are defined for a steel hammer's drop movement. Shorter time increments are used when contact has started between the hammer and specimen. However, solution time extends in this situation. Finally, the value of time increments is decided as 2×10^{-8} s in the numerical analysis.

Numerical analyses for all specimens are performed by considering the changes in concrete compressive strength, drop height, stirrup, and CFRP strip spacing in the software to verify experimental results. Only the weight of the hammer is taken constant in the analyses. After completing numerical analyses by a high technology computer, acceleration, displacement, residual displacement, and impact load values are determined from the software. Numerical results are comparatively given with experimental results in Table 6. Average values between results are also presented to reveal the relationship between the experimental program and numerical analysis. Furthermore, time histories of acceleration, displacement, and impact load values are shown with experimental values in Figures 20–22.

When the relationship between maximum acceleration values of experimental and numerical results is investigated, it is seen that ratios differ between 0.91 and 1.17. Besides, the average ratio of maximum acceleration values is calculated as 1.04. So, only a 4% difference was obtained between results. While the average ratio of experimental displacement values to numerical analysis values is determined as 1.06, the average ratio increases to 1.09 when residual displacements are compared. However, the biggest difference between experimental and numerical results is obtained from impact load values with a value of 19%. The average ratio between results is obtained as 0.81. Support conditions in the experimental study and variation of analysis conditions between numerical models are considered to be the main reasons for the error rates between experimental and numerical results. Besides, concrete material is modeled as homogenous in the software. However, test specimens are nonhomogenous in the experimental study. Environmental conditions, curing operation vibration operations affect the homogeneity of the concrete. It is also considered that the neglecting of the strain rate effect in concrete subjected to dynamic loading leads to the differences between residual displacement values obtained by experiments and numerical analysis. In the current CDP material model, the strain rate dependency of stress–strain behavior of concrete in the tension and compression has been defined with the user's tabular data. The user should provide lots of stress–strain curves generated for different strain rate values predicted in this definition approach. However, strain rates belonging to concrete sections, which are occurred under the dynamic load, are not known at the initial. Authors have recommended that it is required the CDP model must be rearranged to allow for stress–strain behaviors to be defined as a function of strain rate in contrast to the tabular data presented for limited strain-rate values. This means that stress–strain curves belonging to the tension and compression can be modified for whole sections of the structural element by considering that strain rates occurred due to the dynamic load during the explicit analysis.

In the numerical study's final step, the specimens' damage patterns are obtained from the software. For this purpose, the DAMAGET function of the software that gives reliable results in terms of damage development under impact loading is utilized. In this way, damage distributions of the specimens in the experimental study are obtained after numerical analyses. Damage patterns of the specimens are presented in Figure 23. It's seen that fractures are usually concentrated around the area where impact loading is applied in the specimens. Besides, impact energy on the specimens also affects the localization of fractures.

5 | CONCLUSIONS

This study focused on the dynamic response and the reinforced concrete beam's failure modes to column connections strengthened with CFRP strips subjected to impact loading. The beam to column connection test specimens, of which shear-deficient beam parts were strengthened with CFRP strips, had been tested under the effect of impact loading using the drop-weight test setup specially designed by authors for the impact experiments. Detailed literature review revealed a considerable number of studies where impact behavior of beam, column, and slab has been investigated. However, no study related to the reinforced concrete beam's impact behavior to column connections was strengthened with CFRP. It is considered that the experimental data obtained in this study will make important contributions to the literature on the behavior of reinforced concrete structures under impact loading. The results of the study were briefed below.

- The strengthening technique with CFRP strips applied to the beam to column connection test specimens has been successful and enhanced impact performance by improving the impact behavior. The decrease of the intervals between the CFRP strips in the strengthening

procedure where CFRP strips were bonded to the RC beam to column test specimens increased the maximum acceleration values at beam-ends and decreased all displacements measured.

- It has been found out that the maximum strain value measured from CFRP strips is, on average, 2.3 times greater than 0.005 mm/mm, which is the value for the debonding of CFRP strips from the concrete surface in the static loading and exist in the ACI 440 Committee Report. These experimental results unveiled that CFRP strips bear greater shear forces without debonding in the dynamic loading than the static loading, and they exhibit better performance in impulsive loads
- The shear reinforcement ratios of the RC beam to column connections' beam parts have been effective on test specimens' impact responses. The decrease of the shear reinforcement ratios decreased the RC beam's impact performance to column connections and influenced negatively. The acceleration, maximum displacement, and the maximum strain values measured from test specimens have increased with the shear reinforcement ratio decrease. The increase of the maximum strains measured from CFRP strips has led to forced CFRP strips with the greater shear forces.
- The increase of the concrete compressive strength enhanced impact-resistance of the beam to column connection test specimens and improved their impact behavior. With the increase of the concrete compressive strength, the maximum acceleration values increased, whereas all maximum displacements and the maximum strain values decreased.
- The increase of the input impact energy applied to test specimens increased the maximum accelerations, the maximum values of the measured all displacements, the maximum strains. The increase of the input impact energy led to increased contact force transmitted to test specimens. Therefore, when the test specimens were forced with the greater loads, they damaged more and exhibited lower performance under impact loading.
- When the relationship between maximum acceleration values of experimental and numerical results is investigated, it is seen that ratios differ between 0.91 and 1.17. Besides, the average ratio of maximum acceleration values is calculated as 1.04. So, only a 4% difference was obtained between results. While the average ratio of experimental displacement values to numerical analysis values is determined as 1.06, the average ratio increases to 1.09 when residual displacements are compared. When the numerical and experimental results are compared, it is seen that the finite element model created by using ABAQUS finite element software gives successful results in harmony with the experimental results at the design level.

DATA AVAILABILITY STATEMENT

No data, models, or code were generated or used during the study.

ORCID

Özgür Anil https://orcid.org/0000-0002-1939-0366

REFERENCES

1. Do TV, Pham TM, Hao H. Dynamic responses and failure modes of bridge columns under vehicle collision. Eng Struct. 2018a;156:243–59.
2. Do TV, Pham TM, Hao H. Numerical investigation of the behavior of precast concrete segmental columns subjected to vehicle collision. Eng Struct. 2018b;156:375–93.
3. Wang X, Zhang Y, Su Y, Feng Y. Experimental investigation on the effect of reinforcement ratio to capacity of RC column to resist lateral impact loading. Syst Eng Proc. 2011;1:35–41.
4. Bhatti AQ, Kishi N, Mikami H, Ando T. Elasto-plastic impact response analysis of shear-failure-type RC beams with shear rebars. Mater Des. 2009;30:502–10.
5. Jiang H, Wang X, He S. Numerical simulation of impact tests on reinforced concrete beams. Mater Des. 2012;39:111–20.
6. Kishi N, Mikami H, Matsuoka KG, Ando T. Impact behavior of shear-failure-type RC beams without shear rebar. Int J Impact Eng. 2002;27:955–68.
7. Li H, Chen W, Hao H. Influence of drop weight geometry and interlayer on impact behavior of RC beams. Int J Impact Eng. 2019;131:222–37.
8. Zhao DB, Yi WJ, Kunnath SK. Numerical simulation and shear resistance of reinforced concrete beams under impact. Eng Struct. 2018;166:387–401.
9. Fan W, Liu B, Huang X, Sun Y. Efficient modeling of flexural and shear behaviors in reinforced concrete beams and columns subjected to low-velocity impact loading. Eng Struct. 2019a;195:22–50.
10. Anıl Ö, Erdem RT, Tokgöz MN. Investigation of lateral impact behavior of RC columns. Comput Concr. 2018;22:123–32.
11. Anil Ö, Yilmaz MC, Barmaki W. Experimental and numerical study of RC columns under lateral low-velocity impact load. In: Proceedings of the Institution of Civil Engineers—Structures and Buildings; 2018. p. 1–19.
12. Cai J, Ye JB, Chen QJ, Liu X, Wang YQ. Dynamic behaviour of axially-loaded RC columns under horizontal impact loading. Eng Struct. 2018;168:684–97.
13. Demartino C, Wu JG, Xiao Y. Response of shear-deficient reinforced circular RC columns under lateral impact loading. Int J Impact Eng. 2017;109:196–213.
14. Kantar E, Erdem RT, Anıl Ö. Nonlinear finite element analysis of impact behavior of concrete beam. Math Comput Appl. 2011;16:183–93.
15. Liu B, Fan W, Guo W, Chen B, Liu R. Experimental investigation and improved FE modeling of axially-loaded circular RC columns under lateral impact loading. Eng Struct. 2017;152:619–42.
16. Othman H, Marzouk H. Finite-element analysis of reinforced concrete plates subjected to repeated impact loads. J Struct Eng. 2017;143:1–16.

17. Othman H, Marzouk H. Applicability of damage plasticity constitutive model for ultra-high performance fibre-reinforced concrete under impact loads. Int J Impact Eng. 2018;114:20–31.
18. Rajput A, Iqbal MA. Impact behavior of plain, reinforced and pre-stressed concrete targets. Mater Des. 2017;114:459–74.
19. Thilakarathna HMI, Thambiratnam DP, Dhanasekar M, Perera N. Numerical simulation of axially loaded concrete columns under transverse impact and vulnerability assessment. Int J Impact Eng. 2010;37:1100–12.
20. Yılmaz T, Kiraç N, Anil Ö. Experimental investigation of axial loaded reinforced concrete square column subjected to lateral low-velocity impact loading. Struct Concr. 2019;20:1358–78.
21. Yılmaz MC, Anıl Ö, Alyavuz B, Kantar E. Load displacement behavior of concrete beam under monotonic static and low velocity impact load. Int J Civil Eng. 2014;12:488–503.
22. Zhao W, Qian J. Resistance mechanism and reliability analysis of reinforced concrete columns subjected to lateral impact. Int J Impact Eng. 2020;136:103413.
23. Zineddin M, Krauthammer T. Dynamic response and behavior of reinforced concrete slabs under impact loading. Int J Impact Eng. 2007;34:1517–34.
24. Ahmadi H, Liaghat G. Analytical and experimental investigation of high velocity impact on foam core sandwich panel. Polym Compos. 2019;40:2258–72.
25. Anıl Ö, Durucan C, Erdem RT, Yorgancılar MA. Experimental and numerical investigation of reinforced concrete beams with variable material properties under impact loading. Constr Build Mater. 2016;125:94–104.
26. Fujikake K, Soeum S, Matsui T. CFRP strengthened RC beams subjected to impact loading. Proc Eng. 2017;210:173–81.
27. Kantar E, Anıl Ö. Low velocity impact behavior of concrete beam strengthened with CFRP strip. Steel Compos Struct. 2012;12:207–30.
28. Pham TM, Hao H. Impact behavior of FRP-strengthened RC beams without stirrups. J Compos Constr. 2016a;20:1–13.
29. Pham TM, Hao H. Review of concrete structures strengthened with FRP against impact loading. Structure. 2016b;7:59–70.
30. Rubio-González C, José-Trujillo E, Rodríguez-González JA, Mornas A, Talha A. Low-velocity impact behavior of glass fiber-MWCNT/polymer laminates exposed to seawater and distilled water aging. Polym Compos. 2020;41:2181–97. https://doi.org/10.1002/pc.25530
31. Sabet AR, Beheshty MH, Rahimi H. High velocity impact behavior of GRP panels containing coarse-sized sand filler. Polym Compos. 2008;29:932–8.
32. Tai NH, Liu HK, Chen ZC. Compression after impact (CAI) strength of concrete cylinders reinforced by non-adhesive filament wound composites. Polym Compos. 2000;21:268–80.
33. Yılmaz T, Anıl Ö. Low velocity impact behavior of shear deficient RC beam strengthened with CFRP strips. Steel Compos Struct J. 2015;19:417–39.
34. Aghdamy S, Thambiratnam DP, Dhanasekar M. Experimental investigation on lateral impact response of concrete-filled double-skin tube columns using horizontal-impact-testing system. Exp Mech. 2016;56:1133–53.
35. Aoude H, Dagenais FP, Burrell RP, Saatcioglu M. Behavior of ultra-high performance fiber reinforced concrete columns under blast loading. Int J Impact Eng. 2015;80:185–202.
36. Fan W, Shen D, Yang T, Shao X. Experimental and numerical study on low-velocity lateral impact behaviors of RC, UHPFRC and UHPFRC-strengthened columns. Eng Struct. 2019b;191:509–25.
37. Li J, Hao H, Wu C. Numerical study of precast segmental column under blast loads. Eng Struct. 2017;134:125–37.
38. Mutalib AA, Mussa MH, Hao H. Effect of CFRP strengthening properties with anchoring systems on P-I diagrams of RC panels under blast loads. Constr Build Mater. 2019;200:648–63.
39. Shakir AS, Guan ZW, Jones SW. Lateral impact response of the concrete filled steel tube columns with and without CFRP strengthening. Eng Struct. 2016;116:148–62.
40. Wei J, Li J, Wu C. An experimental and numerical study of reinforced conventional concrete and ultra-high performance concrete columns under lateral impact loads. Eng Struct. 2019;201:109822.
41. Xu J, Wu C, Xiang H, Su Y, Li Z. Behaviour of ultra high performancefibre reinforced concrete columns subjected to blast loading. Eng Struct. 2016;118:97–107.
42. Zhang F, Wu C, Zhao XL, Heidarpour A, Li Z. Experimental and numerical study of blast resistance of square CFDST columns with steel-fibre reinforced concrete. Eng Struct. 2017;149:50–63.
43. Zhang X, Hao H. Improved impact resistant capacity of segmental column with fibre reinforced polymer wrap. Int J Impact Eng. 2019;125:117–33.
44. Zhang X, Hao H, Li C. Experimental investigation of the response of precast segmental columns subjected to impact loading. Int J Impact Eng. 2016;95:105–24.
45. Anıl Ö, Kantar E, Yılmaz MC. Low velocity impact behavior of RC slab have different support type. Constr Build Mater. 2015;93:1078–88.
46. Radnić J, Matešan D, Grgić N, Baloević G. Impact testing of RC slabs strengthened with CFRP strips. Compos Struct. 2015;121:90–103.
47. Thai DK, Kim SE. Numerical simulation of pre-stressed concrete slab subjected to moderate velocity impact loading. Eng Fail Anal. 2017;79:820–35.
48. Yılmaz T, Erdem RT. Experimental investigation of impact behaviour of RC slab with different reinforcement ratios. KSCE J Civil Eng. 2020;24:241–54.
49. Yılmaz T, Kıraç N, Anil Ö, Erdem RT, Sezer C. Low velocity impact behaviour of RC two way slab strengthening with CFRP strips. Constr Build Mater. 2018;186:1046–63.
50. Al-Rifaie A, Guan ZW, Jones SW, Wang Q. Lateral impact response of end-plate beam-column connections. Eng Struct. 2017;151:221–34.
51. Eurocode 2. Design of concrete structures—Part 1-1. General rules and rules for buildings; 1992.
52. ASTM. Standard specification for deformed and plain carbon-steel bars for concrete reinforcement. West Conshohocken: ASTM International; 2016.
53. ACI. ACI Committee Report 440, ACI 440.2R-08. Guide for the design and construction of externally bonded FRP systems for strengthening concrete structures. Michigan: American Concrete Institute; 2008.
54. Bao X, Li B. Residual strength of blast damaged reinforced concrete columns. Int J Impact Eng. 2010;37:295–308.
55. Fujikake K, Aemlaor P. Damage of reinforced concrete columns under demolition blasting. Eng Struct. 2013;55:116–25.
56. Kyei C, Braimah A. Effects of transverse reinforcement spacing on the response of reinforced concrete columns subjected to blast loading. Eng Struct. 2017;142:148–64.

57. Wu KC, Li B, Tsai KC. Residual axial compression capacity of localized blast-damaged RC columns. Int J Impact Eng. 2011; 38:29–40.
58. Liao W, Li M, Zhang W, Tian Z. Experimental studies and numerical simulation of behavior of RC beams retrofitted with HSSWM-HPM under impact loading. Eng Struct. 2016;149: 131–46. https://doi.org/10.1016/j.engstruct.2016.07.040
59. ABAQUS. User's manual, version 6.12. Netherlands: SIMULIA Dassault Systèmes Simulia Corp; 2015.
60. Mander JB, Priestley MJN, Park R. Theoretical stress-strain model for confined concrete. J Struct Eng. 1989;114:1804–26.
61. Fan W, Yuan W, Yang Z, Fan Q. Dynamic demand of bridge structure subjected to vessel impact using simplified interaction model. J Bridg Eng. 2011;16:117–26.
62. Malvar LJ, Ross CA. Review of strain rate effects for concrete in tension. ACI Mater J. 1998;95:735–9.
63. Riedel W, Thoma K, Hiermaier S, Schmolinske E. Penetration of reinforced concrete by BETA-B-500, numerical analysis using a new macroscopic concrete model for hydrocodes. In: Proceedings of (CD-ROM) 9 Internationales Symposium, Interaction of the Effects of Munitions with Structures, Berlin Strausberg; 1999. p. 315–322.
64. Sha Y, Hao H. Laboratory tests and numerical simulations of barge impact on circular reinforced concrete piers. Eng Struct. 2013;46:593–605.
65. Kamali AZ. Shear strength of reinforced concrete beams subjected to blast loading [master thesis]. Stockholm, Sweden: Royal Institute of Technology (KTH), Department of Civil and Architectural Engineering, Division of Structural Engineering and Bridges; 2012.

AUTHOR BIOGRAPHIES

Turgut Kaya, MSc,
Lecturer of Civil Engineering Department, Batman University, Batman, Turkey.
turgut.kaya@batman.edu.tr

Murat Aras, PhD,
Student, Research Assistant of Civil Engineering Department, Bilecik Şeyh Edebali University, Bilecik, Turkey.
murat.aras@bilecik.edu.tr

Tolga Yilmaz, PhD,
Research Assistant of Civil Engineering Department, Eskisehir Osmangazi University, Eskisehir, Turkey.
tyilmaz@ktun.edu.tr

Dr. Özlem Çalişkan, PhD,
Assistant Professor, Civil Engineering Department, Bilecik Şeyh Edebali University, Bilecik, Turkey.
ozlem.caliskan@bilecik.edu.tr

Dr. Özgür Anil, PhD,
Professor, Civil Engineering Department, Gazi University, Ankara, Turkey.
oanil@gazi.edu.tr

R. Tuğrul Erdem, PhD,
Associate Professor, Doctoral of Civil Engineering Department, Manisa Celal Bayar University, Manisa, Turkey.
tugrul.erdem@bayar.edu.tr

How to cite this article: Kaya T, Aras M, Yilmaz T, Çalişkan Ö, Anil Ö, Erdem RT. Investigation of impact behavior of reinforced concrete beam to column connection strengthened with carbon fiber-reinforced polymer strips. Structural Concrete. 2021;22:1977–2010. https://doi.org/10.1002/suco.202000571